(12) INTERNATIONAL APPLICATION PUBLISHED UNDER THE PATENT COOPERATION TREATY (PCT)

(19) World Intellectual Property Organization
International Bureau

(43) International Publication Date
31 August 2017 (31.08.2017)

WIPO | PCT

(10) International Publication Number
WO 2017/147044 A1

(51) International Patent Classification:
A61K 38/00 (2006.01)

(21) International Application Number:
PCT/US2017/018645

(22) International Filing Date:
21 February 2017 (21.02.2017)

(25) Filing Language: English

(26) Publication Language: English

(30) Priority Data:
62/298,216 22 February 2016 (22.02.2016) US

(71) Applicant: **INDIANA UNIVERSITY RESEARCH AND TECHNOLOGY CORPORATION** [US/US]; 518 Indiana Avenue, Indianapolis, Indiana 46202 (US).

(72) Inventors: **SRINIVASAN, Mythily**; 354 Wakefield Trace, Greenwood, Indiana 46142 (US). **LAHIRI, Debomoy**; 10674 McClain Drive, Brownsburg, Indiana 46112 (US).

(74) Agents: **ADDISON, Bradford G.** et al.; BARNES & THORNBURG LLP, 11 South Meridian Street, Indianapolis, Indiana 46204 (US).

(81) Designated States *(unless otherwise indicated, for every kind of national protection available)*: AE, AG, AL, AM, AO, AT, AU, AZ, BA, BB, BG, BH, BN, BR, BW, BY, BZ, CA, CH, CL, CN, CO, CR, CU, CZ, DE, DJ, DK, DM, DO, DZ, EC, EE, EG, ES, FI, GB, GD, GE, GH, GM, GT, HN, HR, HU, ID, IL, IN, IR, IS, JP, KE, KG, KH, KN, KP, KR, KW, KZ, LA, LC, LK, LR, LS, LU, LY, MA, MD, ME, MG, MK, MN, MW, MX, MY, MZ, NA, NG, NI, NO, NZ, OM, PA, PE, PG, PH, PL, PT, QA, RO, RS, RU, RW, SA, SC, SD, SE, SG, SK, SL, SM, ST, SV, SY, TH, TJ, TM, TN, TR, TT, TZ, UA, UG, US, UZ, VC, VN, ZA, ZM, ZW.

(84) Designated States *(unless otherwise indicated, for every kind of regional protection available)*: ARIPO (BW, GH, GM, KE, LR, LS, MW, MZ, NA, RW, SD, SL, ST, SZ, TZ, UG, ZM, ZW), Eurasian (AM, AZ, BY, KG, KZ, RU, TJ, TM), European (AL, AT, BE, BG, CH, CY, CZ, DE, DK, EE, ES, FI, FR, GB, GR, HR, HU, IE, IS, IT, LT, LU, LV, MC, MK, MT, NL, NO, PL, PT, RO, RS, SE, SI, SK, SM, TR), OAPI (BF, BJ, CF, CG, CI, CM, GA, GN, GQ, GW, KM, ML, MR, NE, SN, TD, TG).

Declarations under Rule 4.17:

— *of inventorship (Rule 4.17(iv))*

Published:

— *with international search report (Art. 21(3))*

— *before the expiration of the time limit for amending the claims and to be republished in the event of receipt of amendments (Rule 48.2(h))*

[Continued on next page]

(54) Title: PEPTIDES AND METHODS FOR TREATMENT OF NEURODEGENERATIVE DISEASES

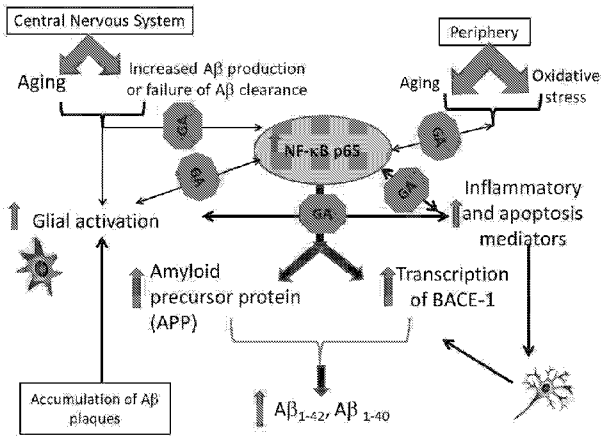

FIG. 7

(57) Abstract: The present disclosure provides pharmaceutical compositions comprising rationally designed peptide analogs of the p65-TAD binding region of GILZ to selectively sequester activated p65. Structural and functional analyses suggest that select GILZ analog (GA) bind p65-TAD with optimum affinity, exhibit an estimated half minimal lethal dose comparable to known peptide drugs and suppress Aβ1-42 induced cytotoxicity. Furthermore, the present disclosure provides uses and methods of using the pharmaceutical compositions, and uses and methods of using pharmaceutical formulations comprising the pharmaceutical compositions, for the treatment of neurodegenerative diseases such as Alzheimer's Disease, Parkinson's Disease, multiple sclerosis, and amyotrophic lateral sclerosis (ALS).

WO 2017/147044 A1

— *with sequence listing part of description (Rule 5.2(a))*

PEPTIDES AND METHODS FOR TREATMENT OF NEURODEGENERATIVE DISEASES

GOVERNMENT RIGHTS

This invention was made with government support under TR000006 awarded by the National Institutes of Health. The government has certain rights in the invention.

CROSS-REFERENCE TO RELATED APPLICATIONS

This application claims the benefit under 35 USC § 119(e) of U.S. Provisional Application Serial No. 62/298,216, filed on February 22, 2016, the entire disclosure of which is incorporated herein by reference

SEQUENCE LISTING

The instant application contains a Sequence Listing which has been submitted electronically in ASCII format and is hereby incorporated by reference in its entirety. Said ASCII copy, created on February 21, 2017, is named 29920-260033_SL.txt and is 8,402 bytes in size.

BACKGROUND

The burden of neurodegenerative pathologies including Parkinson's and Alzheimer's disease (AD) is increasing exponentially worldwide. An accumulating body of evidence suggests that a combination of age related changes in the central nervous system (CNS) with excessive or prolonged inflammatory responses contribute to the pathophysiology of neurodegeneration, synaptic dysfunction and hippocampal behavior deficits in neurodegenerative diseases. In the United States, an estimated 5.1 million Americans currently have AD. The number is projected to increase by 40%, affecting 7.1 million individuals over 65 years of age, by 2025. Translated into healthcare costs, currently the direct cost of caring for AD is estimated at $226 billion and is projected to reach $1.1 trillion by 2050. Thus, there is an urgent need to grow the therapeutic pipeline for AD with agents capable of slowing the disease progression.

The pleiotropic transcription factor, nuclear factor-kappa B (NF-κβ) is induced by many physiological and pathological stimuli in the CNS. The NF-κβ family consists of five members, p50, c-rel, p65, RelB and p52 that can diversely combine to form transcriptionally active dimers. It has been suggested that the nature of the dimers determine

the effects of activated NF-κβ. While c-rel containing dimers preferentially promote transactivation of anti-apoptotic factors, activation of p65/p50 dimers primarily enhance inflammatory and pro-apoptotic gene transcription. Positive and negative regulatory mechanisms maintain a balance between the neuroprotective c-rel dimers and the predominantly deleterious p65:p50 dimers in healthy CNS.

In AD, secondary stimuli such as accumulating beta amyloid and oxidative stress increase activation of p65:p50 dimers in glial cells. The extracellular amyloid plaques mainly include the 42-residue long Aβ amyloid b-peptide (Aβ), obtained by proteolytic cleavage from the much larger amyloid precursor protein (APP). APP is thought to play a role in cellular adhesion and motility. In the amyloidogenic pathway, APP is first cleaved by the β-secretase at the amino-terminus generating soluble sAPPβ and a carboxy-terminal fragment, which is then cleaved by γ-secretase producing the $A\beta_{1-42}$ peptides. Cleavage of APP by β-secretase (also known as beta site amyloid precursor protein cleaving enzyme-1 (BACE-1)) is considered to be the rate limiting step for Aβ generation.

The promoter region of human BACE-1 gene exhibits κB binding elements that physically interact with NF-κβ p65. Activation of NF-κβ p65 increases endogenous BACE-1 transcription and consequent Aβ production. Increased presence of activated p65 and BACE-1 has been observed around Aβ plaques in postmortem AD tissues. Extracellular Aβ peptides predominantly activate p65:p50 dimers in glia and post-mitotic neurons and enhance transactivation of inflammatory and pro-apoptotic genes. Increased presence of IL-1β, IL-6, and TNF-α have been reported in the affected tissues, serum and CSF of AD patients. Elevated Bax (proapoptotic) to Bcl-2 (anti-apoptotic) ratio have been observed in Aβ stimulated neuronal cells. A feed-back loop of excessive Aβ accumulation, NF-κβ activation, cytotoxicity and more Aβ production culminate in neurodegeneration. Conditional knock out of p65 has been shown to attenuate BACE-1 transcription and Aβ genesis in AD mice. Absence of p65 co-factors such as p300/CREB binding associated factor has been shown to mediate resistance to Aβ induced toxicity. Thus, although neuronal p65 has been shown to contribute to the physiological functions of synapse formation and transmission, considerable evidence suggest that excessive activated p65 in the CNS lead to neurodegenerative pathology. Hence selective inhibition of activated p65 could ameliorate pathologies wherein inflammation is closely associated with degeneration, such as AD.

Structurally, p65 has an amino terminal rel homology domain (RHD), a nuclear localization sequence (NLS) masked by the IκB inhibitory complex and a carboxy terminal transactivation domain (TAD). The transactivation activity of p65 is mediated by

interactions of the TAD with co-regulators and the basal transcription machinery. Glucocorticoid induced leucine zipper (GILZ) is a p65 binding protein that sequesters activated p65 and inhibits transactivation of inflammatory and apoptotic factors. Mutational and binding analyses localized the interaction interface to the proline rich carboxy terminus of GILZ and the TAD of p65. Molecular modeling suggested that the p65 binding domain of GILZ adopts a flexible polyproline type II (PP_{II}) helical conformation that interacts with the highly conserved F^{534}/F^{542} in p65-TAD.

In recent years, considerable success has been achieved in the development of structurally engineered peptide analogs of the binding epitope(s) of a protein as therapeutic leads. The strategy is increasingly adopted in the design of mimics of proline rich motif that mediate transient intermolecular interactions. The specificity of the interaction is determined by the nature of the proline rich binding domain interface.

Thus, there exists a need for novel pharmaceutical compositions and pharmaceutical formulations for the treatment of neurodegenerative diseases. The present disclosure provides pharmaceutical compositions comprising rationally designed peptide analogs of the p65-TAD binding region of GILZ to selectively sequester activated p65. Structural and functional analyses suggest that select GILZ analog (GA) bind p65-TAD with optimum affinity, exhibit an estimated half minimal lethal dose comparable to known peptide drugs and suppress Aβ1-42 induced cytotoxicity. Furthermore, the present disclosure provides uses and methods of using the pharmaceutical compositions, and uses and methods of using pharmaceutical formulations comprising the pharmaceutical compositions, for the treatment of neurodegenerative diseases such as Alzheimer's Disease, Parkinson's Disease, multiple sclerosis, and amyotrophic lateral sclerosis (ALS).

BRIEF DESCRIPTION OF THE DRAWINGS

FIGURES 1A-1F show comparative modeling of GILZ analogs. Superimposition of human delta sleep inducing peptide (DSIP; PDB: 1DIP) with the predicted model of human GILZ (FIG. 1A), superimposition of indicated analog (blue) with the critical residues in the proline glutamic acid rich region of human GILZ model (red) (FIGS 1B-1F). Structural similarity in terms of root mean square deviation (RMSD) for each superimposition is indicated.

FIGURES 2A-2F show the docked complex of wild type GILZ-PER (proline glutamic acid rich region) or GILZ analog (GA) with human p65-TAD. Representative

molecular model of p65-TAD docked (blue) with wild type GILZ-PER (FIG. 2A) and indicated analog (FIG. 2B-2F) (red) are shown. The residues in each analog <5Å distance of highly conserved residues in p65-TAD2 (Phe or Phe) and the "LXXLL" motif in p65-TAD_1 that suggest proximity with residues critical for transcriptional activity are shown.

FIGURES 3A-3F show GA-rp65 binding analysis. Binding between the plate-bound GILZ analog (GA) or control peptide (CP) (20μM-640μM) at increasing concentration and the r-p65 was detected with the anti-DDK as described in the methods section. A dose dependent decrease in percent bound r-p65 was observed in association with the GA (FIG. 3A). Scatchard plot analysis of bound p65 $(A_0 - A)/(A_0)$ against the ratio of bound p65 to free GA ($y= (A_0 - A)/(A_0)/[(A_0 - A)/(A_0)/(a_0-i_0)]$ was used to determine the dissociation constant for the interaction between indicated GA and r-p65 (FIG. 3B-3F).

FIGURES 4A and 4B show the effect of GILZ analog (GA) on cellular morphology and metabolic activity in neuroblasts. Differentiated SK-N-SH neuroblastoma cultures were exposed to individual GA or control peptide (CP) at the indicated concentration for 24 hours. (FIG. 4A). Phase contrast imaging of the cells shows no apparent adverse effects on morphology of cells exposed to GA-1 or GA-2 or CP- 1 or CP-2 at either concentration. Exposure to CP-3 at both concentrations showed morphological changes consistent with cell death. (FIG. 4B). Cell lysates were assessed by CTG assay to determine relative levels of intracellular ATP. An increase in Relative Luminescence Units (RLU) suggesting cellular viability was observed with all treatments except CP-3.

FIGURES 5A-5G show the effect of GA on lactate dehydrogenase (LDH) release. U373 MG astroglioma cells were exposed to increasing concentrations of indicated GILZ analog (GA) or control peptide (CP) (0.5 μM to 1mM) for 24 hours. The release of LDH into the cell culture supernatant from damaged cells was measured. Percentage of LDH was calculated as the ratio of the difference between the peptide treated and untreated cells to that of the difference between the positive control and the untreated cells (FIG. 5A). The IC50 was determined by logarithmic extrapolation (FIG. 5C-5G). Flow cytometric analysis of Annexin positive U373 cells treated as indicated was determined as a measure of apoptosis (FIG. 5B).

FIGURES 6A-6E show the effect of GILZ analog (GA) treatment on human fetal brain cells. Primary cultures of HFB (Div 17) were exposed to Aβ1-42 and treated with 50μM of indicated GA or control peptide (CP). Cytoplasmic extracts of cells collected at 24 hours was assessed for viability by CTG assay. Data are presented as ΔRLU (difference in relative luminescent units (RLU) between the Aβ1-42 exposed cells and unexposed cells)

(FIG. 6A, FIG. 6B). Culture medium collected at 24 hrs was assessed for indicated cytokines (FIG. 6C, FIG. 6D). Effect of GA on NF-κβ activation. Primary cultures of HFB exposed to Aβ1-42 (10μg/ml) and treated with indicated GA or CP as above were harvested at the end of 4 hours. 5μg of nuclear extract was tested for binding of the activated p65 NF-κB subunit to an NF-κB consensus sequence using the Trans AM NF-κB ELISA kit. The p65 DNA binding activity was calculated as the ratio of absorbance from Aβ1-42 stimulated cells to that of unstimulated cells (FIG. 6E). Values are the average/-S.D. *=p<0.05 as compared to Aβ1-42 exposed cells, @=p<0.05 as compared with Aβ1-42 and CP-1 or CP-2 treated cultures

FIGURE 7 shows the Schematic representation of pathological mechanisms of AD and points of intervention by GA. Increased oxidative stress and other age related changes upregulate NF-κB p65 which in turn increase transcription of amyloid precursor protein (APP) and/or beta site amyloid precursor protein cleaving enzyme-1 (BACE-1) leading to generation and accumulation of Aβ peptides in the CNS parenchyma. Glial cells exposed to Aβ peptides exhibit increased p65 activation and secrete inflammatory and apoptosis mediators. Affected neurons upregulate Aβ peptides and the vicious cycle of Aβ deposition, inflammation and neuronal apoptosis leads to AD. GILZ analogs (GA) by virtue of binding activated NF-κB p65 blocks Aβ generation and suppressing inflammation, thereby ameliorating AD pathology.

FIGURE 8 shows comparative modeling and docking of PGA:p65 (A-B). Superimposition of indicated PGA (blue) with the critical proline rich region of human GILZ (red), both built using PDB:1DIP as template. Root mean square deviation (RMSD) representing structural similarity is given. (C-D) Representative model of p65-TAD (blue) docked with indicated PGA (red). The p65-TAD residues critical for transcriptional activity at close proximity (RMSD <5Å) to PGA are highlighted.

FIGURES 9A and 9B show binding between plate-bound PGA (20^M-640^M) and r-p65 (15pg/ml). (FIG. 9A) All PGA exhibit a dose dependent decrease in %bound r-p65. (FIG. 9B). Scatchard plot analysis of bound p65 against the ratio of bound p65 to free PGA-4 (representative) to determine KD. A:absorbance of PGA:p65, Ao: absorbance of r-p65- DDKanti-DDK in the absence of bound PGA, ao: total PGA concentration and io: total r-p65concentration.

FIGURES 10A and 10B show U373 cells were exposed to increasing concentrations of different PGA or wild type GILZ-P (0.5μM to 500μM) for 24 hours. Percent LDH released into the medium was calculated as the ratio of the difference in PGA

treated to untreated cells to that of the difference between the positive control and untreated cells (FIG. 10A). The IC_{50} was determined by logarithmic extrapolation (FIG. 10B).

FIGURES 11A-11D show primary cultures of HFB pretreated with indicated PGA at IC_{50} concentration was exposed to vehicle or 10μM of $A\beta_{1-42}$. Cell viability at 24 hours was assessed by CTG assay. Data are presented as ΔRLT (difference in relative luminescent units) between Aβ1-42 exposed and unexposed cells) (FIG. 11A, FIG. 11B). Culture medium was assessed for IL-6 (FIG. 11C). HFB cultured similarly was harvested at the end of 4 hours (FIG. 11D). Activated p65 in nuclear extract was tested for binding an NF-κB consensus sequence. The p65 DNA binding activity was calculated as the ratio of absorbance from $A\beta_{1-42}$ stimulated cells to that of unstimulated cells. Data are mean/-S.D. *=$p<0.05$.

FIGURE 12 shows a weighted rank order based on parameters of known peptide drugs suggested that the PGA-2 and PGA-4 exhibit significant drug like properties.

FIGURES 13A-13E show HFNC cultures at DIV20. A phase contrast image (FIG. 13A) and nuclear staining with DAPI (FIG. 13B) are displayed. In FIG. 13C, 13D, and 13E, cells labelled with indicated antibody and merged image. Pan-neuronal antibody, a cocktail of mAbs, identifies somatic, nuclear, dendritic and axonal proteins distributed across the pan neuronal architecture. Significant individual and co-labeling with pan-neuronal and anti-GFAP mAb suggests presence of immature neural stem cells as well as both differentiated neurons and astrocytes. Arrows and arrowheads point to cells labeled only with pan-neuronal mixture or anti-GFAP respectively.

The following numbered embodiments are contemplated for the present disclosure and are non-limiting:

1. A pharmaceutical composition comprising a polypeptide from about 8 to about 12 amino acid residues, the polypeptide comprising a tetrapeptide having the sequence of PXXP, wherein

P is proline; and

X is any amino acid.

2. The pharmaceutical composition of clause 1, wherein the polypeptide comprises a sequence of Formula I: X1-X2-X3-P-X4-X5-P-X6-X7, wherein each of X1, X2, X3, X4, X5, X6, and X7 is independently any amino acid.

3. The pharmaceutical composition of clause 2, wherein X1 is E.

4. The pharmaceutical composition of clause 2, wherein X1 is A.

5. The pharmaceutical composition of any of clauses 2 to 4, wherein X2 is P.

6. The pharmaceutical composition of any of clauses 2 to 4, wherein X2 is A.

7. The pharmaceutical composition of any of clauses 2 to 6, wherein X3 is A.

8. The pharmaceutical composition of any of clauses 2 to 6, wherein X3 is L.

9. The pharmaceutical composition of any of clauses 2 to 6, wherein X3 is K.

10. The pharmaceutical composition of any of clauses 2 to 9, wherein X4 is selected from the group consisting of R, L, E, A, and Y.

11. The pharmaceutical composition of any of clauses 2 to 10, wherein X5 is selected from the group consisting of Q, A, and S.

12. The pharmaceutical composition of clause 1, wherein the polypeptide comprises a sequence of XXXPXXPXX.

13. The pharmaceutical composition of clause 12, wherein the polypeptide comprises a sequence of EPAPXXPXX (SEQ ID NO: 1).

14. The pharmaceutical composition of clause 12, wherein the polypeptide comprises a sequence of EPLPXXPXX (SEQ ID NO: 2).

15. The pharmaceutical composition of clause 12, wherein the polypeptide comprises a sequence of EAAPXXPXX (SEQ ID NO: 3).

16. The pharmaceutical composition of clause 12, wherein the polypeptide comprises a sequence of APAPXXPXX (SEQ ID NO: 4).

17. The pharmaceutical composition of clause 12, wherein the polypeptide comprises a sequence of APKPXXPXX (SEQ ID NO: 5).

18. The pharmaceutical composition of clause 1, wherein the polypeptide comprises a sequence of Formula II: X1-X2-X3-P-X4-X5-P-X6-X7-X8,
wherein each of X1, X2, X3, X4, X5, X6, X7, and X8 is independently any amino acid.

19. The pharmaceutical composition of clause 18, wherein X1 is E.

20. The pharmaceutical composition of clause 18, wherein X1 is A.

21. The pharmaceutical composition of any one of clauses 18 to 20, wherein X2 is P.

22. The pharmaceutical composition of any one of clauses 18 to 20, wherein X2 is A.

23. The pharmaceutical composition of any one of clauses 18 to 22, wherein X3 is A.

24. The pharmaceutical composition of any one of clauses 18 to 22, wherein X3 is L.

25. The pharmaceutical composition of any one of clauses 18 to 22, wherein X3 is K.

26. The pharmaceutical composition of any one of clauses 18 to 25, wherein X4 is selected from the group consisting of R, L, E, A, and Y.

27. The pharmaceutical composition of any one of clauses 18 to 26, wherein X5 is selected from the group consisting of Q, A, and S.

28. The pharmaceutical composition of clause 1, wherein the polypeptide comprises a sequence of XXXPXXPXXX.

29. The pharmaceutical composition of clause 28, wherein the polypeptide comprises a sequence of EPAPXXPXXX (SEQ ID NO: 6).

30. The pharmaceutical composition of clause 28, wherein the polypeptide comprises a sequence of EPLPXXPXXX (SEQ ID NO: 7).

31. The pharmaceutical composition of clause 28, wherein the polypeptide comprises a sequence of EAAPXXPXXX (SEQ ID NO: 8).

32. The pharmaceutical composition of clause 28, wherein the polypeptide comprises a sequence of APAPXXPXXX (SEQ ID NO: 9).

33. The pharmaceutical composition of clause 28, wherein the polypeptide comprises a sequence of APKPXXPXXX (SEQ ID NO: 10).

34. The pharmaceutical composition of clause 1, wherein the polypeptide comprises a sequence of EPAPRQPAT (SEQ ID NO: 11).

35. The pharmaceutical composition of clause 1, wherein the polypeptide comprises a sequence of EPAPRAPEG (SEQ ID NO: 12).

36. The pharmaceutical composition of clause 1, wherein the polypeptide comprises a sequence of EPAPLAPYG (SEQ ID NO: 13).

37. The pharmaceutical composition of clause 1, wherein the polypeptide comprises a sequence of EPAPRAPGT (SEQ ID NO: 14).

38. The pharmaceutical composition of clause 1, wherein the polypeptide comprises a sequence of EPAPRAPDG (SEQ ID NO: 15).

39. The pharmaceutical composition of clause 1, wherein the polypeptide comprises a sequence of EPLPEAPDT (SEQ ID NO: 16).

40. The pharmaceutical composition of clause 1, wherein the polypeptide comprises a sequence of EPAPESPQV (SEQ ID NO: 17).

41. The pharmaceutical composition of clause 1, wherein the polypeptide comprises a sequence of EPAPEQPDG (SEQ ID NO: 18).

42. The pharmaceutical composition of clause 1, wherein the polypeptide comprises a sequence of APAPASPQV (SEQ ID NO: 19).

43. The pharmaceutical composition of clause 1, wherein the polypeptide comprises a sequence of EAAAESPQV (SEQ ID NO: 20).

44. The pharmaceutical composition of clause 1, wherein the polypeptide comprises a sequence of APAPAAPET (SEQ ID NO: 21).

45. The pharmaceutical composition of clause 1, wherein the polypeptide comprises a sequence of EAAAEAAET (SEQ ID NO: 22).

46. The pharmaceutical composition of clause 1, wherein the polypeptide comprises a sequence of EPAPEAPEGY (SEQ ID NO: 23).

47. The pharmaceutical composition of clause 1, wherein the polypeptide comprises a sequence of EPAPYQPEG (SEQ ID NO: 24).

48. The pharmaceutical composition of clause 1, wherein the polypeptide comprises a sequence of EPAYEAQET (SEQ ID NO: 25).

49. The pharmaceutical composition of clause 1, wherein the polypeptide comprises a sequence of EPAPEAGET (SEQ ID NO: 26).

50. The pharmaceutical composition of clause 1, wherein the polypeptide comprises a sequence of EPAPEAPET (SEQ ID NO: 27).

51. The pharmaceutical composition of clause 1, wherein the polypeptide comprises a sequence of EPAPESPQV (SEQ ID NO: 17).

52. The pharmaceutical composition of clause 1, wherein the polypeptide comprises a sequence of EPAPYQPRG (SEQ ID NO: 28).

53. The pharmaceutical composition of clause 1, wherein the polypeptide comprises a sequence of APKPYQPRG (SEQ ID NO: 29).

54. The pharmaceutical composition of clause 1, wherein the polypeptide consists essentially of a sequence of EPAPRQPAT (SEQ ID NO: 11).

55. The pharmaceutical composition of clause 1, wherein the polypeptide consists essentially of a sequence of EPAPRAPEG (SEQ ID NO: 12).

56. The pharmaceutical composition of clause 1, wherein the polypeptide consists essentially of a sequence of EPAPLAPYG (SEQ ID NO: 13).

57. The pharmaceutical composition of clause 1, wherein the polypeptide consists essentially of a sequence of EPAPRAPGT (SEQ ID NO: 14).

58. The pharmaceutical composition of clause 1, wherein the polypeptide consists essentially of a sequence of EPAPRAPDG (SEQ ID NO: 15).

59. The pharmaceutical composition of clause 1, wherein the polypeptide consists essentially of a sequence of EPLPEAPDT (SEQ ID NO: 16).

60. The pharmaceutical composition of clause 1, wherein the polypeptide consists essentially of a sequence of EPAPESPQV (SEQ ID NO: 17).

61. The pharmaceutical composition of clause 1, wherein the polypeptide consists essentially of a sequence of EPAPEQPDG (SEQ ID NO: 18).

62. The pharmaceutical composition of clause 1, wherein the polypeptide consists essentially of a sequence of APAPASPQV (SEQ ID NO: 19).

63. The pharmaceutical composition of clause 1, wherein the polypeptide consists essentially of a sequence of EAAAESPQV (SEQ ID NO: 20).

64. The pharmaceutical composition of clause 1, wherein the polypeptide consists essentially of a sequence of APAPAAPET (SEQ ID NO: 21).

65. The pharmaceutical composition of clause 1, wherein the polypeptide consists essentially of a sequence of EAAAEAAET (SEQ ID NO: 22).

66. The pharmaceutical composition of clause 1, wherein the polypeptide consists essentially of a sequence of EPAPEAPEGY (SEQ ID NO: 23).

67. The pharmaceutical composition of clause 1, wherein the polypeptide consists essentially of a sequence of EPAPYQPEG (SEQ ID NO: 24).

68. The pharmaceutical composition of clause 1, wherein the polypeptide consists essentially of a sequence of EPAYEAQET (SEQ ID NO: 25).

69. The pharmaceutical composition of clause 1, wherein the polypeptide consists essentially of a sequence of EPAPEAGET (SEQ ID NO: 26).

70. The pharmaceutical composition of clause 1, wherein the polypeptide consists essentially of a sequence of EPAPEAPET (SEQ ID NO: 27).

71. The pharmaceutical composition of clause 1, wherein the polypeptide consists essentially of a sequence of EPAPESPQV (SEQ ID NO: 17).

72. The pharmaceutical composition of clause 1, wherein the polypeptide consists essentially of a sequence of EPAPYQPRG (SEQ ID NO: 28).

73. The pharmaceutical composition of clause 1, wherein the polypeptide consists essentially of a sequence of APKPYQPRG (SEQ ID NO: 29).

74. The pharmaceutical composition of clause 1, wherein the polypeptide consists of a sequence of EPAPRQPAT (SEQ ID NO: 11).

75. The pharmaceutical composition of clause 1, wherein the polypeptide consists of a sequence of EPAPRAPEG (SEQ ID NO: 12).

76. The pharmaceutical composition of clause 1, wherein the polypeptide consists of a sequence of EPAPLAPYG (SEQ ID NO: 13).

77. The pharmaceutical composition of clause 1, wherein the polypeptide consists of a sequence of EPAPRAPGT (SEQ ID NO: 14).

78. The pharmaceutical composition of clause 1, wherein the polypeptide consists of a sequence of EPAPRAPDG (SEQ ID NO: 15).

79. The pharmaceutical composition of clause 1, wherein the polypeptide consists of a sequence of EPLPEAPDT (SEQ ID NO: 16).

80. The pharmaceutical composition of clause 1, wherein the polypeptide consists of a sequence of EPAPESPQV (SEQ ID NO: 17).

81. The pharmaceutical composition of clause 1, wherein the polypeptide consists of a sequence of EPAPEQPDG (SEQ ID NO: 18).

82. The pharmaceutical composition of clause 1, wherein the polypeptide consists of a sequence of APAPASPQV (SEQ ID NO: 19).

83. The pharmaceutical composition of clause 1, wherein the polypeptide consists of a sequence of EAAAESPQV (SEQ ID NO: 20).

84. The pharmaceutical composition of clause 1, wherein the polypeptide consists of a sequence of APAPAAPET (SEQ ID NO: 21).

85. The pharmaceutical composition of clause 1, wherein the polypeptide consists of a sequence of EAAAEAAET (SEQ ID NO: 22).

86. The pharmaceutical composition of clause 1, wherein the polypeptide consists of a sequence of EPAPEAPEGY (SEQ ID NO: 23).

87. The pharmaceutical composition of clause 1, wherein the polypeptide consists of a sequence of EPAPYQPEG (SEQ ID NO: 24).

88. The pharmaceutical composition of clause 1, wherein the polypeptide consists of a sequence of EPAYEAQET (SEQ ID NO: 25).

89. The pharmaceutical composition of clause 1, wherein the polypeptide consists of a sequence of EPAPEAGET (SEQ ID NO: 26).

90. The pharmaceutical composition of clause 1, wherein the polypeptide consists of a sequence of EPAPEAPET (SEQ ID NO: 27).

91. The pharmaceutical composition of clause 1, wherein the polypeptide consists of a sequence of EPAPESPQV (SEQ ID NO: 17).

92. The pharmaceutical composition of clause 1, wherein the polypeptide consists of a sequence of EPAPYQPRG (SEQ ID NO: 28).

93. The pharmaceutical composition of clause 1, wherein the polypeptide consists of a sequence of APKPYQPRG (SEQ ID NO: 29).

94. The pharmaceutical composition of any one of clauses 1 to 93, wherein the composition suppresses p65 binding.

95. The pharmaceutical composition of any one of clauses 1 to 93, wherein the composition suppresses p65 activation.

96. The pharmaceutical composition of any one of clauses 1 to 93, wherein the composition inhibits NF-κB translocation to the nucleus of a cell.

97. A pharmaceutical formulation comprising the pharmaceutical composition of any one of clauses 1 to 96.

98. The pharmaceutical formulation of clause 97 further comprising a pharmaceutically acceptable carrier.

99. The pharmaceutical formulation of clause 97 or clause 98 optionally including one or more other therapeutic ingredients.

100. The pharmaceutical formulation of any one of clauses 97 to 99 wherein the formulation is a single unit dose.

101. A lyophilisate or powder of the pharmaceutical formulation of any one of clauses 97 to 100.

102. An aqueous solution produced by dissolving the lyophilisate or powder of clause 101 in water.

103. Use of the pharmaceutical composition or the pharmaceutical formulation of any one of clauses 1-100 for the treatment of a neurodegenerative disease in a patient.

104. The use of clause 103 wherein the neurodegenerative disease is Alzheimer's Disease.

105. The use of clause 103 wherein the neurodegenerative disease is Parkinson's Disease.

106. The use of clause 103 wherein the neurodegenerative disease is multiple sclerosis.

107. The use of clause 103 wherein the neurodegenerative disease is amyotrophic lateral sclerosis (ALS).

108. A method of treating a neurodegenerative disease in a patient, said method comprising the step of administering the pharmaceutical composition or the pharmaceutical formulation of any one of clauses 1-100 to the patient in need thereof.

109. The method of clause 108 wherein the neurodegenerative disease is Alzheimer's Disease.

110. The method of clause 108 wherein the neurodegenerative disease is Parkinson's Disease.

111. The method of clause 108 wherein the neurodegenerative disease is multiple sclerosis.

112. The method of clause 108 wherein the neurodegenerative disease is amyotrophic lateral sclerosis (ALS).

In particular, the following analogs were developed and evaluated:

Analog	**Sequence**	**SEQ ID NO:**	**Name**
Analog 1	EPAPRQPAT	11	
Analog 2	EPAPRAPEG	12	
Analog 3	EPAPLAPYG	13	PGA-2
Analog 4	EPAPRAPGT	14	
Analog 5	EPAPRAPDG	15	
Analog 6	EPLPEAPDT	16	
Analog 7 (GA-4)	EPAPESPQV	17	PGA-4
Analog 8 (GA-5)	EPAPEQPDG	18	PGA-5
Analog 9	APAPASPQV	19	
Analog 10	EAAAESPQV	20	
Analog 11	APAPAAPET	21	
Analog 12	EAAAEAAET	22	
Analog 13	EPAPEAPEGY	23	
Analog 14 (GA-3)	EPAPYQPEG	24	PGA-3
Analog 15	EPAYEAQET	25	
Analog 16	EPAPEAGET	26	
Analog 17	EPAPEAPET	27	
Analog 18	EPAPESPQV	17	
Analog 19	EPAPYQPRG	28	
Analog 20 (GA-1)	APKPYQPRG	29	PGA-1

Furthermore, the following analogs were tested:

Name	Sequence	SEQ ID NO:
PGA-1	APKPYQPRG	29
PGA-2	EPAPLAPYG	13
PGA-3	EPAPYQPEG	24
PGA-4	EPAPESPQV	17
PGA-5	EPAPEQPDG	18

Increased NF-κB p65 secondary to aging and environmental stimuli contribute significantly to the inflammation and degeneration in AD. Synthetic compounds including terpenoids like adenanthin and resveratrol or other sirtuin activators interact with NF-κB p65, suppress inflammation and cytotoxicity in AD models. As opposed to high throughput screening, computational design of interface peptide mimics followed by functional evaluation represents an efficient method in the drug design and discovery process. Here we report the design and physicochemical characteristics of peptide analogs of the GILZ:p65 interface, show that select analogs bind p65-TAD and suppress Aβ induced toxicity in human fetal brain cells exhibiting potential therapeutic value for AD.

In human interactome, preponderant transient intermolecular interactions are mediated by proline rich epitope of one protein binding the aromatic residue rich flat interface of the second protein. Often the proline rich epitope adopts an extended PP_{II} helical conformation that behaves as an adaptable glove in obtaining the correct binding orientation. Here it is pertinent to note that the template based modeling suggested that the p65 binding domain of GILZ exhibits a PP_{II} helical conformation and that the p65-TAD is unstructured or flat. Mutational analyses identified ^{120}PEA(S)P^{124} of GILZ as hot spot residues for interacting with NF-κB p65. In the GILZ:p65-TAD complex, the critical proline of GILZ, ^{120}P exhibits φ and ψ angles of -67° ±5° of 142.5° ± 15° respectively and is in close proximity with the conserved phenylalanines (^{534}F, ^{542}F) of p65-TAD. Collectively, these observations suggest that the GILZ:p65-TAD complex represents a druggable target for development of specific therapeutic leads.

Incorporating rational substitutions in the polyproline motif of GILZ in the context of the p65- TAD interface we designed multiple peptide analogs of GILZ or GA. Molecular superposition is one of the most important means to interpret the relations between three-dimensional structures. The low RMSD upon superimposition with experimental PP_{II} and wild type GILZ suggests that the select GA represent true structural mimic of the p65 binding domain of GILZ. Significantly docking analyses showed that the top ranked GA

exhibited >20% contact with the functionally critical p65-TAD residues (F^{534}, F^{542}) in >90% of docked solutions.

An important advantage of proline-rich motif at interface of transient intermolecular interactions is the weak binding kinetics without compromising affinity. Furthermore, it allows for introduction of small changes in the sequence of the motif or its binding domain to mediate large changes in the affinity of the interaction. We observed that the GA-1 and GA-2 evaluated by functional analysis exhibited greater affinity for binding r-p65 than the full length r- GILZ. Previously, proline rich peptides that bind Src homology 3 binding domain or the transcription factor human estrogen receptor alpha or the cell surface CD80 ligand have been shown to exhibit dissociation constant (K_D) in the micromolar range and inhibit protein:protein interactions.

Many peptide drugs including copaxone, leuprolide acetate/goserelin (peptide antagonists of GnRH receptor), octreotide (a cyclic octapeptide mimicking natural hormone somatostatin) and glucagon like peptide-1(GLP-1) analog have been evaluated in models of AD substantiating the credibility of peptide drugs for AD. Proline rich PP_{II} helical peptides such as apidaecin, oncocin and drosocin have shown to exhibit significant influx into CNS and distribution within the brain parenchyma. Hence PGA is likely to cross the blood brain barrier and reach optimal concentration in the brain to be clinically efficient. Significantly, the estimated LD50 for GA-1 and GA-2 as determined by the method of Speilmann et al. is within the range of these peptide drugs. Furthermore the ability of GA-1 and GA-2 to suppress Aβ induced inflammatory and cytotoxic responses in human fetal brain cells suggests potential as AD therapeutic agents.

The goal of biological therapies is to restore healthy balance by targeting specific molecules that are critical for mediating or perpetuating imbalanced cellular responses. In recent years peptide-based drugs have gained considerable value in the discovery phase of drug development, in particular in the design of interface mimotopes. The functionally active peptides are amenable to further modifications into peptidomimetic compounds or small molecules with improved pharmacokinetic properties. In this context, the low molecular weight GA-1 and GA-2 can act as lead compounds in the development of specific small molecule inhibitors of NF-κβ p65 with significant therapeutic potential for chronic neurodegenerative diseases including AD (see FIG. 7).

In some embodiments, the pharmaceutical formulations described herein further comprise a pharmaceutically acceptable carrier. In some embodiments, the pharmaceutical formulations described herein further comprise a pharmaceutically acceptable

diluent. Diluent or carrier ingredients used in the pharmaceutical compositions containing polypeptides can be selected so that they do not diminish the desired effects of the polypeptide. Examples of suitable dosage forms include aqueous solutions of the polypeptides, for example, a solution in isotonic saline, 5% glucose or other well-known pharmaceutically acceptable liquid carriers such as alcohols, glycols, esters and amides.

As used herein, "carrier" refers to any ingredient other than the active component(s) in a formulation. Pharmaceutically acceptable carriers are determined in part by the particular composition being administered, as well as by the particular method used to administer the composition (see, e.g., Remington's Pharmaceutical Sciences, 17th ed. (1985)). The choice of carrier will to a large extent depend on factors such as the particular mode of administration, the effect of the carrier on solubility and stability, and the nature of the dosage form. In one illustrative aspect, the carrier is a liquid carrier.

As used herein, the term "pharmaceutically acceptable" includes "veterinarily acceptable", and thus includes both human and animal applications independently. For example, a "patient" as referred to herein can be a human patient or a veterinary patient, such as a domesticated animal (e.g., a pet).

In some embodiments, the pharmaceutical formulations described herein optionally include one or more other therapeutic ingredients. As used herein, the term "active ingredient" or "therapeutic ingredient" refers to a therapeutically active compound, as well as any prodrugs thereof and pharmaceutically acceptable salts, hydrates, and solvates of the compound and the prodrugs. Other active ingredients may be combined with the described polypeptides and may be either administered separately or in the same pharmaceutical formulation. The amount of other active ingredients to be given may be readily determined by one skilled in the art based upon therapy with described polypeptides.

In some embodiments, the pharmaceutical formulations described herein are a single unit dose. As used herein, the term "unit dose" is a discrete amount of the composition comprising a predetermined amount of the described polypeptides. The amount of the described polypeptides is generally equal to the dosage of the described polypeptides which would be administered to an animal or a convenient fraction of such a dosage such as, for example, one-half or one-third of such a dosage.

In one illustrative aspect, parenteral formulations may be suitably formulated as a sterile non-aqueous solution or as a dried form to be used in conjunction with a suitable vehicle such as sterile, pyrogen-free water. The preparation of parenteral formulations under sterile conditions, for example, by lyophilization, may readily be accomplished using

standard pharmaceutical techniques well known to those skilled in the art.

The aqueous preparations according to the invention can be used to produce lyophilisates by conventional lyophilization or powders. The preparations according to the invention are obtained again by dissolving the lyophilisates in water or other aqueous solutions. The term "lyophilization," also known as freeze-drying, is a commonly employed technique for presenting proteins which serves to remove water from the protein preparation of interest. Lyophilization is a process by which the material to be dried is first frozen and then the ice or frozen solvent is removed by sublimation in a vacuum environment. An excipient may be included in pre-lyophilized formulations to enhance stability during the freeze-drying process and/or to improve stability of the lyophilized product upon storage. For example, see Pikal, M. Biopharm. 3(9)26-30 (1990) and Arakawa et al., Pharm. Res., 8(3):285-291 (1991).

In one embodiment, the solubility of the polypeptides used in the preparation of a parenteral formulation may be increased by the use of appropriate formulation techniques, such as the incorporation of solubility-enhancing agents.

In various embodiments, formulations for parenteral administration may be formulated to be for immediate and/or modified release. Modified release formulations include delayed, sustained, pulsed, controlled, targeted and programmed release formulations. Thus, a polypeptide may be formulated as a solid, semi-solid, or thixotropic liquid for administration as an implanted depot providing modified release of the active compound.

The formulations can be presented in unit-dose or multi-dose sealed containers, such as ampules and vials. The formulations can also be presented in syringes, such as prefilled syringes.

In various embodiments, the dosages of the polypeptides can vary significantly depending on the patient condition and the severity of the disease to be treated. The effective amount to be administered to a patient is based on body surface area, patient weight or mass, and physician assessment of patient condition.

Suitable dosages of the polypeptides can be determined by standard methods, for example by establishing dose-response curves in laboratory animal models or in humans in clinical trials. Illustratively, suitable dosages of polypeptides (administered in a single bolus or over time) include from about 1 pg/kg to about 10 μg/kg, from about 1 pg/kg to about 1 μg/kg, from about 100 pg/kg to about 500 ng/kg, from about 1 pg/kg to about 1 ng/kg, from about 1 pg/kg to about 500 pg/kg, from about 100 pg/kg to about 500 ng/kg,

from about 100 pg/kg to about 100 ng/kg, from about 1 ng/kg to about 10 mg/kg, from about 1 ng/kg to 1 mg/kg, from about 1 ng/kg to about 1 μg/kg, from about 1 ng/kg to about 500 ng/kg, from about 100 ng/kg to about 500 μg/kg, from about 100 ng/kg to about 100 μg/kg, from about 1 μg/kg to about 500 μg/kg, or from about 1 μg/kg to about 100 μg/kg. In each of these embodiments, dose/kg refers to the dose per kilogram of a patient's or animal's mass or body weight.

The present disclosure provides uses and methods of using the pharmaceutical compositions, and uses and methods of using pharmaceutical formulations comprising the pharmaceutical compositions, for the treatment of neurodegenerative diseases such as Alzheimer's Disease, Parkinson's Disease, multiple sclerosis, and amyotrophic lateral sclerosis (ALS).

EXAMPLES

EXAMPLE 1

Peptides and reagents: All GILZ peptides were synthesized as peptide amides with amino- terminal acetylation (Genescript, Piscataway, NJ) at 95% purity as confirmed by mass spectrometry. To facilitate intracellular delivery the GA were either co-synthesized with the cell penetrating agent, TAT (transactivator of transcription) peptide or used as covalent mixture with Pep-1 chariot peptide (Anaspec, Fremont,CA). Recombinant human p65 protein (r-p65) with DDK tag (catalog number TP320780), purified recombinant human GILZ protein (r-GILZ) with GST tag and biotinylated anti-DDK antibody were from Ori-Gene Technologies Inc., Rockville, MD. Purified $A\beta_{1-42}$ peptide was purchased from American Peptide company (American peptide company, Sunnyvale, CA: Product # 62-0-80 Lot # 1310160T). $A\beta_{1-42}$ peptide stock (1 mg/mL) was prepared in cell culture medium and incubated at 37°C for 24 hours prior to use in cell cultures.

Comparative modeling: Models of human GILZ and its mimics were built by the CPH models and Geno3D servers using delta sleep inducing peptide (DSIP-PDB:1DIP) as template based on > 90% sequence similarity. While the Geno3D system builds models based on 'topology mapping, the CPH system uses profile-based alignment as seed for developing energy-minimized homology model. The secondary structure assignment of the GILZ models was independently assessed by the PROSS (Protein dihedral angle-based Secondary Structure assignment) program. Superimposition of the model of each GILZ mimic with experimentally determined PP_{II} helix and wild type GILZ determined the similarity between the structures in terms of root mean square deviation (RMSD). Homology models of p65-TAD was developed similarly using elongation factor eEF3 (PDB:3H7H) as template with which it shares 42% sequence similarity.

Design and modeling of GILZ mimic: Strategies to determine the smallest biologically active fragment of a lead peptide involves truncation, deletion, alanine scanning and substitution of residues. Deletion studies suggested that the amino terminal helix of GILZ is critical for dimerization but is not involved in the interaction with NF-κβ. Truncation mutants suggested that the residues spanning ^{120}P-P^{127} of the GILZ were critical for GILZ mediated inhibition of NF-κβ transactivation. Molecular modeling showed that the GILZ-COOH or a 22 residue peptide derived from the proline rich region adopted an extended PP_{II} helical conformation and interacted with the p65-TAD exhibiting weak binding kinetics. Alanine scanning mutagenesis suggested that the substitution of the ^{120}PXXP^{123} motif

abrogated the ability to inhibit NF-κβ transactivation potentially due to loss of PP_{II} conformation. In human and mouse GILZ, hydrogen bonding between the side chain of Ser or Thr and the backbone carbonyl of Glu or Pro respectively could contribute to the stability of PP_{II} conformation. We designed 40 GILZ mimics by incorporating rational substitutions in the p65 binding motif of GILZ with residues that increase the propensity for PP_{II} helical conformation and stabilize it. Comparative modeling with substituted residues for all 40 GA was performed to obtain structural representation of each with reference to the adjacent residues of human GILZ. In addition we introduced conformational constraints by superimposing each GILZ mimic model on structures with solved or experimental PP_{II} helix and wild type human GILZ to select for mimics with significant structural homology (see FIGS. 1A-1F). The PP_{II} content of GILZ mimics as determined by PROSS ranged from 14.3%, 28.6% and 42.9%. Since PP_{II} helix formation is a locally driven event with little/no involvement of long-range interactions, it is logical to presume that the synthetic GILZ mimetic peptide with blocked end groups will adopt a similar conformation as in the predicted model. Twenty GILZ mimics that exhibit near structural congruence with DSIP (<1Å) or wild type GILZ or experimentally determined PP_{II} structure (<2Å) were selected for *in silico* docking.

EXAMPLE 2

GILZ:p65-TAD docking: Models of human GILZ or GILZ mimic and the p65-TAD were applied as probe and target respectively in PatchDock, a geometry based algorithm that yields docked transformations scored on the basis of molecular shape complementarity and atomic desolvation energy. Top one thousand solutions were refined using FireDock (Fast Interaction Refinement in molecular docking), a program that optimizes binding of the probe by restricting side-chain flexibility to clashing interface residues. The refined docking solutions were scored based on softened van der Waals interactions, atomic contact energy, electrostatic and additional binding free energy estimations. The top ranked solutions so obtained were further screened using Chimera for interatomic distance of <5Å between the residues of GILZ mimic and the functionally critical residues of p65-TAD. The solution with most contacts was further refined by FlexPepDock using the wild type GILZ:p65-TAD complex with greater than 50% intermolecular residue contacts as reference.

Docking of GILZ mimic and p65-TAD: To be of potential therapeutic value, the GILZ mimic should adopt PP_{II} helical conformation in the context of the critical binding residues in p65- TAD. The p65-TAD is commonly divided into two distinct regions, TAD-

1521-551 consisting of 36 amino acids and TAD-2428-520 with 92 residues. It has been reported that the TAD_1 accounts for nearly 95% of the transactivation potential of full-length p65 and that the TAD2 alone is less potent mediating about 30% activation. In particular, the highly conserved aromatic residues (F^{534}, F^{542}), acidic residues (D^{531},D^{533}) and phosphorylation sites (Ser^{529},$Ser^{536)}$ in p65-TAD1 have been identified as critical for transactivation.

Homology model of p65-TAD was built using solution structure of the elongation factor eEF3 (PDB: 2XI3, 2WI3) with which it shares 42% sequence similarity. The spatial orientations of wild type GILZ and top 20 GILZ mimics with p65-TAD were assessed by multiple docking algorithms. One thousand interaction possibilities identified by rigid-docking algorithm were improved by coarse refinement to restrict side-chain flexibility at the interface. The docked complexes were ranked using an optimized global energy function for higher probability prediction. Top ten solutions of each GILZ mimic were evaluated for proximity to p65-TAD residues. In general two residues are considered in contact with each other if the distance between the CP atoms is <5Å. Interactions between the conserved F^{534}-F^{542} in the p65-TADi and the critical prolines P^{120}/ P^{123} of GILZ could promote C-H$\cdots\pi$ interaction and provide substantial binding energy in the GILZ:p65-TAD complex. All solutions that exhibited an RMSD of <5Å with the critical F^{534} and F^{542} were selected for further screening (Table 1).

Table 1. Characteristics of GILZ mimics

		Superimposition		p65-Transactivation Domain			
	% PPII	PPII	GILZ model	% TA1	% TA2		
					CR-1	CR-2	CR-3
				521-531	435-455	462-479	491-505
PGA-1	14.3	0.82	0.216	19	43	39	20
PGA-2	42.9	0.531	0.216	18	32	13	9
PGA-3	14.3	0.109	0.428	11	14	23	4
PGA-4	14.3	1.049	0.482	4	13	47	29
PGA-5	28.6	1.234	0.586	11	14	23	4
PGA-6	14.3	0.844	0.645	21	54	34	9
PGA-7	14.3	0.156	0.681	30	20	0	11
PGA-8	14.3	1.72	0.842	15	41	32	5
PGA-9	42.9	0.257	0.88	24	42	29	13
PGA-10	28.6	0.161	0.9	12	38	23	7
PGA-11	28.6	0.703	0.912	20	46	23	6
PGA-12	42.9	1.17	1	10	12	18	6
PGA-13	14.3	0.58	1.018	3	35	55	6
PGA-14	28.6	1.172	1.033	32	28	10	2
PGA-15	14.3	0.391	1.047	12	36	8	7
PGA-16	14.3	0.252	1.154	18	38	33	1
PGA-17	28.6	1.293	1.227	15	25	24	9
PGA-18	14.3	1,248	1.243	16	24	31	22
PGA-19	28.6	0.581	1.49	7	22	24	7
PGA-20	42.9	1.174	1.613	37	43	9	2

Table 1 shows the characteristics of twenty GILZ mimics: GILZ models (GM) with substituted residues at the proline rich region of wild type GILZ sequence were developed using Geno3D and CPHModels. Each GA model was superimposed over wild type GILZ and experimentally determined polyproline (PP_{II}) helical structures. The root mean square deviation (RMSD) of each superimposition as a measure of structural similarity is shown. Each GM was docked with the molecular model of p65-TAD and the docked complexes were screened for interface p65-TAD residues within 5Å distance of GM.

Sixty of the top one hundred predictions of wild type GILZ exhibited close proximity with nearly 50% of p65-TAD_1 residues suggesting near-native interactions (FIG. 2A). The wild type GILZ:p65-TAD complex with the lowest global energy and maximum contacts with p65-TAD was selected as reference for refining each of the 20 GILZ mimic-

p65TAD complexes in two hundred independent FlexPepDock simulations. Significantly ten of the twenty GILZ mimics exhibited interatomic distance of <5Å not only with the conserved phenylalanine in p65-TAD_1 but also with the putative LXXLL motif in p65-TAD_2 (FIGS. 2B and 2C). The LXXLL motif commonly observed in transcription factors are known to mediate protein-protein interactions. A rank order was developed based on percent PPII content, structural similarity with wild type GILZ and percent contact with p65-TAD. We selected two GILZ mimics or analogs (GA-1 and GA-2) that exhibit near native docking, structural congruence with experimental PP_{II} and wild type GILZ and good PP_{II} potential for screening by cellular analyses. In addition we selected one mimic with good PP_{II} potential but fewer contacts with p65-TAD and two GILZ mimics that possess low PP_{II} content but acceptable percent contact with the p65-TAD in docking analyses as control peptides for PP_{II} conformation (control peptide 1) and p65 docking potential (control peptide 2 and control peptide 3) respectively.

EXAMPLE 3

Binding of GILZ and human r-p65: Previously we observed that the r-GILZ exhibits ten times higher affinity than a 22 residue GILZ peptide for r-p65. We used similar method to determine direct binding kinetics of GA hexapeptides with human r-p65. High binding ELISA plates were coated with increasing concentrations of r-GILZ (0.5 μM to 20 μM) or each GA or control peptide (20 μM - 640 μM) and probed with 80pM r-p65 followed by detection with anti- DDK antibody. Absorbance at 650nm was measured with a mixing time of 30s using BIORAD microplate reader. Percent bound p65 was determined considering the binding response of r- GILZ (20pM) with r-p65 as 100%. The dissociation constant of the interaction between the GA or the control peptide and r-p65 was determined by the method of Friguet et al., as described. A fraction of the bound r-p65 (x) and the ratio of bound r-p65 to the free GA or control peptide (y) was determined by the equations: $x = (A_0 - A)/(A_0)$, where A_0 is the absorbance of r- p65anti-p65 complex in the absence of bound GA or control peptide and $y = (A_0 - A)/(a_0 - i_0)x(A_0 - A)/(A_0)$, where a_0 is the total concentration of GA or control peptide and i_0 is the total concentration of r-p65. K_D for the interaction was determined by the Scatchard equation: $x = 1 + K_D/y$.

Kinetics of GA:-p65 interaction: Previously the strength of interaction between rGILZ or wild type GILZ-P and r-p65 has been shown to be $5.91 \pm 2.4 * 10^{-7}$M and $1.12 \pm 0.25 * 10^{-6}$M, respectively. We evaluated the binding kinetics of individual GA at increasing concentrations with the plate bound r-p65 protein at constant concentration. We

observed that the percent bound r-p65 was over 25% with GA-1, GA-2 and CP-1 even at the lowest concentration evaluated (FIG. 3A). The dissociate constant, K_D, as calculated by the method of Friguet et al. was 2.29+/-0.2x10^{-6}M for GA-1 and 3.24+/-0.19x10^{-6}M for GA-2. The strength of interaction of the GA:p65-TAD binding is consistent with other transient protein:peptide interactions such as that of peptide inhibitors of matrix metalloproteinase and that of SMRT peptides binding the BTB domain of BCL6. The control peptides exhibited higher K_D values of 3.27+/-1.8x10^{-6}M, 3.4+/-0.15x10^{-6}M and 4.28+/-0.5 x10^{-6}M for CP-1, CP-2 and CP-3 respectively (FIGS. 3B-3F).

EXAMPLE 4

Cell Titer-Glo (CTG) luminescent cell viability assay: Human neuroblastoma (SK-N-SH) cells cultured in minimal essential medium (MEM) supplemented with 1% fetal bovine serum (FBS) and 1% penicillin (100U/ml)/streptomycin (100µg/ml) were differentiated with 10 µM all-trans retinoic acid for 7 days. After resting for 24 hours in the low serum medium, the cells were seeded in 24 well (10^5 cells/well) culture plates in fresh medium and incubated with 50µM or 500µM of individual GA or control peptide for additional 24 hours. The cultures were then photographed using a phase contrast Leica microscope (Leica Microsystems Inc, Buffalogrove, IL). Subsequently, the cells were harvested, lysed with lysis buffer (M-PER, Pierce) and the lysate was assessed for metabolic activity using the luciferase based CTG assay (CTG, Promega, Madison, WI). Briefly, cell lysate (5µL) in 25µL of phosphate buffered saline was transferred to an opaque white 96-well plate, and then 30µL of CTG assay solution was added. The relative luminescent signal (RLT) was quantified using a Glowmax luminometer (Promega).

Effect of GA on cellular morphology and metabolic activity: Any compound with potential therapeutic effect should be biocompatible and nontoxic. So, we first screened the effects of GA on cellular morphology and viability. Cultures of neuroblasts exposed to 50µM or 500µM of individual GA or CP-1 or CP-2 did not show any change in cell morphology suggesting that the four peptides were not toxic. Exposure to CP-3 at either concentration showed morphological changes consistent with cell death (FIG. 4A). The effect of GA on cellular metabolic activity was assessed by the CTG assay which measures intracellular ATP concentrations as an indicator of actual cell number. The results of the CTG assay were very similar and showed that the two GA and CP-1 and CP-2 did not adversely

affect the differentiated neuroblastoma cells, but treatment with CP-3 reduced the viability of the cells at both concentrations tested (FIG. 4B).

EXAMPLE 5

Lactate dehydrogenase (LDH) assay: To detect direct GA-induced cell lysis we performed LDH release assays (Roche Molecular Diagnostics). Human glioblastoma (U373) cells were maintained in MEM supplemented with 10% FBS and 1% penicillin (100U/ml)/streptomycin (100µg/ml) at 37 °C in 5% CO_2-humidified incubators and sub-cultured once or twice a week. Approximately 5 x 10^4 U373 cells/well were cultured in 96-well plates in the presence of increasing concentrations of individual GA or control peptide from 0.5µM to 500µM. Cells treated with 2% triton-X 100 (Sigma Aldrich, St. Louis, MO) for 10 minutes served as positive control. Untreated cells served as controls for spontaneous LDH-release. Specific LDH-release was calculated according to the following formula: LDH-release %=100*(GA or control peptide treated cells - untreated cells)/(positive control-untreated cells). The IC50 values were extrapolated by logarithmic estimation. The LD_{50} in mg/kg was predicted using the formula, Log (LD_{50}) = 0.506x (log IC_{50}) + 0.475.

Detection apoptosis by flow cytometry: To further assess cell cytotoxicity, the apoptotic effects of individual GA or control peptide was evaluated by the Annexin-V and propidium iodide (PI) dual staining method (Annexin-V-Fluos staining kit, Roche Diagnostics, Mannheim, Germany). As opposed to apoptotic cells, necrotic cells with ruptured cell membrane take up PI, the DNA binding dye. Thus, cells which take up both fluorochromes are a mixture of apoptotic and necrotic cells, whereas cells that exclude PI but bind Annexin V are (early) apoptotic cells. U373 cells cultured with varying concentrations of individual GA or control peptide (0.5µM to 50µM) for 24 hours were centrifuged and suspended in 100µl of Annexin V/PI labelling solution (20µl each of Annexin-V-Fluos labelling reagent and PI in 1ml of binding buffer) for 15min at room temperature. After washing the cells were resuspended in PBS:1% paraformaldehyde and analyzed using a FACScan flow cytometer (BD Biosciences, San Jose, CA).

Effect of GA on membrane integrity and apoptosis: Membrane integrity as a measure of cell survival was assessed by the leakage of intracellular LDH molecules into culture medium. Treatment with GA-1 and GA-2 were best tolerated as indicated by the reduced % LDH release at all concentrations as compared to untreated cultures or cultures exposed to control peptides (FIG. 5A). IC_{50} extrapolated from regression analysis is 226.78 µM for GA-1 and 198.4 µM for GA-2 (FIGS. 5C and 5D). The IC_{50} was lower for CP-1

(49.9 μM), CP-2 (26.58 μM) and CP-3 (26.63 μM) (FIG. 5E-5G). Using the Speilmann method, the LD50 in mg/kg body weight is estimated to be 380.44 for GA-1 and 369.42 for GA-2 and 272.78, 237.52 and 237.62 for CP-1, CP-2 and CP-3, respectively. Many therapeutic peptides such as leuprolide and glatiramer acetate have been shown to exhibit similar LD_{50} values. Furthermore the cytotoxic effect of each peptide at increasing concentration from 0.5 μM to 50 μM was assessed by Annexin and PI staining (FIG. 5B). GA-1 and GA-2 exhibit < 25% apoptosis at highest concentration.

EXAMPLE 6

Functional assays in human primary mixed brain cultures (HFB). Primary cultures of mixed HFB were prepared from the brain parenchyma of aborted fetuses (80-100 days gestational age). The tissues were obtained from the Birth Defects Research Laboratory (BDRL) at the University of Washington, Seattle with approval from the Indiana University Institutional Review Board (IRB). The IRB determined that the use of anonymous human biological materials received from this depository is not considered as human subjects research (supplementary document, s1). The NIH funded BDRL tissue distribution program operates separately in full compliance with all relevant state and federal laws and regulations with donors providing written informed consent.

Fetal brain materials (10-20g) were shipped overnight in chilled Hibernate-E medium (Invitrogen) supplemented with B27 (Invitrogen), GlutaMAX (Invitrogen) and antibiotic- antimycotic solution (Cellgro). HFB were prepared and cultured as described. Briefly, cells were cultured in Neurobasal medium (Invitrogen) without phenol red supplemented with 1xB27, 50mM GlutaMAX, 1xantibiotic cocktail, 5ng/mL recombinant fibroblast growth factor 2 (bFGF) (Invitrogen), and 2μL/mL Normocin (InVivoGen, San Diego, CA, USA). Cells were counted and seeded onto poly-D-lysine (Sigma-Aldrich) coated 24-well plates (Corning, Lowell, MA, USA) at $1.5x10^5$ cells per well and maintained at 37°C in a 5% CO2 incubator. Half media changes were performed every 4th day of culture and morphology was monitored via phase contrast microscopy. Culture medium was removed from cells on day 17 (DIV17) and replaced with Neurobasal medium with B27. Appropriate wells were then added vehicle, or carrier peptide or individual GA or control peptide (at 50 μM) for 30min followed by exposure to $A\beta_{1-42}$ at a final concentration of 10μM/ well and incubated for 4 hours or 48 hours. Cells and conditioned media were harvested and stored for further analysis. Relative ATP concentration was measured using the CTG kit (Promega). Data is presented as ΔRLU=RLU of $A\beta_{1-42}$ exposed cells- RLU unexposed cells. Conditioned

media collected were assessed for specific cytokines using the OptEIA kits (BD Biosciences). Nuclear and cytoplasmic fractions were extracted using the CelLytic™ NuCLEAR™ Extraction Kit (Sigma) following manufacturer's protocol. Five microgram of nuclear extracts was incubated in a 96-well plate coated with oligonucleotides containing the NF-κβ consensus nucleotide sequence (5'-GGGACTTTCC-3') (SEQ ID NO: 30). The activated NF-κβ bound to DNA was detected by anti-p65 antibody followed by a peroxidase coupled secondary antibody and substrate using the TransAM kit protocol (Active Motif). Nuclear extracts of Raji cells was used as the positive control.

Select GA protect against $A\beta_{1-42}$ induced toxicity in human fetal brain cells.

We used an *in-vitro* neurodegeneration model in which primary human fetal brain cells are allowed to mature gradually. The system provides an opportunity to test the pharmacological and toxicological effects of GA on differentiated neurons and glia simultaneously. The relative ATP concentration of GA or control peptide treated HFB cultures in the presence or absence of Aβ1-42 over the cultures exposed to vehicle alone (Δ-RLU) was determined by the CTG assay. Cultures exposed to GA were best tolerated while the cultures treated with CP-2 or CP-3 exhibited significant toxicity (FIG. 6A). The mean RLU of vehicle treated cells varied between 7352.75+/- 1265.2 and 16157.5+/-4950 and the average RLU of cultures exposed to Aβ1-42 varied between 6067.25+/-903.05 and 11574.25+/- 4139.3 in different experiments. The viability was significantly higher in cells exposed to Aβ1-42 and treated with GA-1 or GA-2 (FIG. 6B). Although A-RLU was higher in cultures treated with CP-1, it was not significant when compared to that in untreated Aβ1-42 exposed cultures. The relative concentration of IL-1β and IL-6 was significantly lower in culture medium of cells exposed to Aβ1-42 and treated with GA-1 or GA-2 as compared with that from untreated or cultures treated with the control peptides (FIGS. 6C and 6D).

Select GA treatment inhibits activated p65: Previously Aβ1-42 has been shown to enhance expression of activated NF-κB in glia and post-mitotic neurons. We measured nuclear p65 binding activity using activated NF-κB specific ELISA. Nuclear p65 was significantly higher in cells exposed to Aβ1-42 than in unexposed cells (FIG. 6E). There was a trend towards decreased nuclear p65 in Aβ1-42 exposed cells treated with GA-1 and GA-2 as compared to untreated cells or cells treated with control peptide. No significant difference in nuclear p65 was observed in cells treated only with the peptides in the absence of exposure to Aβ1-42.

Comparative analysis of physical and functional characteristics of known receptor antagonists and peptide drugs in clinical use today with that of GA, suggest that the GA-1 and GA-2 exhibit significant drug like properties (Table 2).

Table 2. Physical and functional characteristics of GILZ analog and control peptides

	Structural similarity RMSD			Docking features				%PPII		# rotatable bonds		Log P		K_D (uM)		LD50 (mM)		% apoptosis at LD50		Overall rank
	Wild type GILZ		PPII peptide	% TA1		%TA2		>25	<25	<10	>10	<5	>5	<3	>3	>100	<100	<25	>25	
	<1	>1	<1	>25	<25	>25	<25													
	1	0	1	1	0	1	0									1	0	1	0	
PGA1	1		1	1			0		0		0		0		0		0		0	3
PGA2	1		1	1		1		1		1		1		1		1		1		10
PGA3	1				0	1			0	1			0		0	1		1		6
PGA4	1		1	1		1		1		1		1			0	1		1		9
PGA5	1		1		0	1			0		0		0		0	1			0	4

EXAMPLE 7

Design and selection of PGA: Human GILZ has an amino terminal α-helix for dimerizing and a carboxy terminal proline glutamic acid rich region for intermolecular interactions. Mutational and binding analyses showed that the proline rich region of GILZ adopts an extended PP_{II} helical conformation and binds the p65- TAD. In the GILZ:p65 complex, interaction between the imino ring of P^{120}/ P^{123} of GILZ and the side chain of F^{534}/ F^{542} in the p65-TAD could promote C-H.π interactions and provide substantial binding energy. Functional studies have shown that the highly conserved $F^{534}$and F^{542} in the transactivation domain are critical for p65 induced transactivation.

Forty PGA were designed by incorporating rational substitutions in the p65 binding domain of GILZ with residues that facilitate PP_{II} formation and stabilization at the interface with the p65-TAD. Homology models of PGA built using delta sleep inducing peptide (DSIP; PDB:1DIP) as template were screened for conformational constraints by superimposing on experimental PP_{II} and wild type human GILZ. The PP_{II} content of all PGA as determined by PROSS method ranged from 14.3%, 28.6% and 42.9%. Since PP_{II} helix formation is often a locally driven event, the synthetic PGA with blocked end groups will likely adopt a similar conformation as in the predicted model. Twenty PGA that exhibit structural congruence with DSIP (<1A), wild type GILZ and experimental PP_{II} structure (<2Å) were selected for docking analysis.

Homology model of p65-TAD was built using elongation factor eEF3 (PDB:3H7H) as template. Spatial orientation of wild type GILZ peptide or each PGA with p65-TAD was assessed by multiple algorithms including rigid-docking based on shape complementarity and coarse refinement methods that restrict side-chain flexibility at interface. The docked complexes were ranked using an optimized global energy function. Significantly most solutions of top ten PGA exhibited close proximity to the phenylalanines (F^{534}, F^{542}) and the putative LXXLL motif in p65-TAD (see FIGS. 9C and 9D). The LXXLL motif in transcription factors has been shown to mediate protein-protein interactions. A rank order developed based on percent PP_{II} content, structural similarity with wild type GILZ and percent contact with p65-TAD identified five PGA with near native docking and good PP_{II} potential. The top five PGA were selected for cellular analyses (see FIG. 8).

EXAMPLE 8

Kinetics of PGA:-p65 interaction: The binding kinetics of top five PGA with full length human r-p65 was assessed as described. Plate bound GILZ-P or PGA at increasing concentrations was probed with r-p65-DDK (Ori-Gene Technologies Inc., Rockville, MD) at constant concentration and detected with anti-DDK. T he percent bound r-p65 increased with increasing concentration of PGA (see FIG. 9A). The dissociation constant, K_D, calculated by the method of Friguet, was lowest for PGA-2 (2.29+/-0.2x10^{-6}M) followed by PGA-4 (3.28+/- 0.2x10^{-6}M), PGA-5 (3.4+/-0.2x10^{-6}M), PGA-3 (3.27+/-1.8x10^{-6}M) and PGA-1 (4.28+/-0.5 x10^{-6}M) (FIG. 9B).

EXAMPLE 9

Effects of PGA on membrane integrity and apoptosis: The top five PGA were covalently synthesized with the cell penetrating TAT (transcriptional transactivation) peptide to facilitate intracellular delivery (Genescript, NJ). Membrane integrity of U373 microglial cells exposed to increasing concentration of each PGA from 0.5μm to 500μM was assessed by the leakage of intracellular lactate dehydrogenase (LDH) into culture medium (Roche, IN).

All five PGA exhibited a dose dependent LDH release (FIG. 10A). IC_{50} extrapolated from regression analysis was highest for PGA-1 (2.27μM) followed by PGA-5 (2.0μM), PGA-2 (1.95μM), PGA4 (1.5μM) and PGA-3 (0.98μM) (FIG. 10B). The cytotoxic effect of each PGA at increasing concentration from 0.5μM to 50μM was also assessed by Annexin and PI staining. PGA-2 and PGA-4 exhibit < 25% apoptosis.

EXAMPLE 10

Select PGA protects against $A\beta_{1-42}$ induced toxicity, prevents p65 activation and cytokine response in human fetal brain (HFB) cells. Primary HFB cells pretreated with vehicle or each PGA at IC_{50} concentration were cultured in the presence of $A\beta_{1-42}$ aggregates (10μM) for 24 hours at 37°C and 5% CO_2. Viability in terms of relative luminescent Units (RLU) was quantified using a Glowmax luminometer (Promega, WI). Data are presented as ARLU=RLU of $A\beta_{1-42}$ exposed cells-RLU of unexposed cells. HFB cultures exposed to PGA-2, PGA-3 and PGA-4 were well tolerated. Cultures treated with PGA-1 and PGA-5 exhibited significant toxicity (FIG. 11A). The mean RLU of vehicle treated HFB varied between 7352.75+/-1265.2 and 16157.5+/-4950. Average RLU of cultures exposed to $A\beta_{1-}$

$_{42}$varied between 6067.25+/-903.05 and 11574.25+/- 4139.3 in different experiments. The viability was significantly higher in HFB cells treated with PGA-2, PGA-3 or PGA-4 and exposed to $A\beta_{1-42}$ (FIG. 11B). The culture supernatants were assessed for cytokines by ELISA (R&D Systems, MN). AIL-1p (not shown) and AIL-6 concentration was significantly lower in PGA-2, PGA-4 or PGA-5 treated cultures over unstimulated or cultures exposed to $A\beta_{1-42}$ alone (FIG. 11C). Primary HFB cultured similarly and harvested at the end of 4 hours was assessed for nuclear p65 using TransAM kit for NF-κB p65 (Active Motif, CA). $A\beta_{1-42}$ exposed cells treated with PGA-2 and PGA-4 exhibited decreased nuclear p65 (FIG. 11D).

EXAMPLE 11

Evaluation of the effect of PGA-2 and PGA-4 on AD-relevant cells. An *in-vitro* neurodegeneration model derived from primary HFNC can be utilized in the instant example. Previously maturing HFNC cultures have been shown to exhibit positive staining for neuronal, glial and synaptic markers. Further, the neuronal population has been shown to increase with time and exhibit physiological activity. In addition the cells are capable of being transfected with external agents providing a tool for evaluating the efficacy of potential drug candidates for CNS pathologies. Importantly, abundant Aβ production and tau proteins make this a powerful model for Alzheimer's research. The effects of PGA-2 and PGA-4 on neuronal and glial cell morphology, BACE-1 and Aβ production in primary HFNC can be evaluated.

HFNC: Briefly, human brain cells derived from aborted fetus (90-110 days gestational age) can be plated in poly D-lysine coated 24-well plates (Sigma, St. Louis, MO) using defined culture medium (Neurobasal medium with 1X B27, 50 mM Glutamax, 1X antibiotics cocktail and recombinant human basic fibroblast growth factor 2 (bFGF) at 5 ng/mL (Gibco, Grand Island, NY) and incubated at 37°C, 5% CO_2. Half media changes can be performed every fourth day and morphology monitored by phase contrast microscopy. The procedure usually results in ~75% pure neurons. Purity of the cultured cells has been demonstrated by visualization of neurons and glia using pan- neuronal antibody (Millipore, Billerica, MA) and glial fibrillary acidic protein (GFAP) (Sigma) respectively.

PGA treatment and immunocytochemistry: PGAs were covalently synthesized with the cell penetrating TA T to facilitate intracellular delivery as peptide amides with amino terminal acetylation. At DIV16 (mixed population of neuronal and glial cells) or DIV20 (predominantly mature neurons) of HFNC, the defined culture

medium can be replaced with Neurobasal medium supplemented only with B27. PGA-2 (168.9μM), PGA-4 (101.7μM) at IC_{50} concentration or TAT peptide (100μM) can be added and the cultures continued to be incubated for 24 hours. The effect on neuronal and glial cell morphology can be assessed by immunostaining using fluorophore conjugated astroglial markers (GFAP) and neuron specific proteins (Nestin, Pan N). Stained sections can be visualized with an inverted fluorescent microscope (Leica Microsystems) and appropriate sets of filters.

Quantitation of BACE-1 and AB: Separate HFNC cultures at Div16 can be added PGA-2, PGA-4 or TAT (carrier). Equal quantity of cDNA isolated from cells harvested after 24 hours can be amplified for BACE-1, APP and reference genes β-2 microglobulin and GAPDH by real time polymerase chain reaction (Applied Biosystems; assay IDs: human BACE-1 (Hs00201573_m1), human APP (Hs01552283_m1), human GAPDH (4333764T), human B2M (4333766T). Fold changes can be calculated using the delta-Ct method normalized to the geometric mean of the reference genes. Levels of $Aβ_{1-40}$ and $Aβ_{1-42}$ in the culture medium can be measured using specific commercially available ELISA kits (Covance, Princeton, NJ). Absolute Aβ values (in pg/ml of culture medium) can be normalized to total protein and scaled relative to levels in untreated cultures.

As PGA-2 or PGA-4 did not affect the morphology of HFNC as seen under inverted bright field microscope, HFNC exposed to either PGA may exhibit significant neuronal staining on day-20 suggesting neuropreservation. Transfection of human brain cells with NF-κB dependent miRNA has been shown to downregulate BACE-1, APP and Aβ production. By blocking p65, PGA-2 and PGA-2 treatment may reduce BACE-1 transcription and consequent Aβ production.

EXAMPLE 12

Investigation of the molecular effects of PGA on AD relevant cells: Accumulating environmental and oxidative stress induces NF-κB p65 activation in neuronal and glial cells contributing to AD pathogenesis. Quantitation of biologically active molecules integrally involved in AD pathology is used as outcome measures in early stages of drug discovery.

Cell culture: HFNC cultures at Div16 added PGA-2 or PGA-4 at IC_{50} or TAT (carrier) as above can be exposed 30 minutes later to H_2O_2 (10μM) or sodium nitroprusside (SNP) (30μM) as radical oxygen or nitric oxide donor respectively for 4 hours or 24 hours.

Some cultures can be added a cell permeable 2',7'-dichlorofluorescin diacetate (DCFH-DA) (10μM) (Molecular Probes, Eugene, OR) probe at the time of PGA treatment to measure reactive oxygen species (ROS). Cells and culture medium can be collected for RNA and protein analysis.

Evaluation of activated NF-κB. cytokines and glutamate: The effect of PGA on p65 transactivation in each cell type can be evaluated by co-labeling of cells harvested at 4 hours using fluorophore conjugated markers for neuron (NSE, Nestin, Pan N), astrocytes (GFAP); microglia (IBA1) and nuclear p65 (Abcam Cambridge, MA) and visualized with an inverted fluorescent microscope. Activated p65 in nuclear fraction of cells can be quantitated by ELISA. IFN-α, IL-iβ and IL-6 and glutamate in culture medium collected at 24 hours can be measured using specific ELISA kits (R&D Systems, MN) and enzymatic assays (BioVision Inc. Milpitas, CA) respectively.

Cytoprotection assays: Fluorescence in cell lysates added DCFH-DA and collected at 4 hours can be measured at 504/529 nm and data expressed as ratio of ROS to total protein. Activated caspase in culture medium can be measured using caspase-3 assay kit (R&D systems). Total protein isolated from cells harvested at 24 hours can be probed by immunoblot (Abcam) for apoptosis related proteins Bax, Bcl-2 and caspase-3 using specific antibodies. Fold changes in these apoptotic proteins transcripts can be determined by polymerase chain reaction arrays (Applied Biosystems; Human TaqMan® Human Apoptosis Array; Cat. # 4414072).

Other neuroprotective agents suppressed caspase-3 and Bax in neuronal cells.Preliminary data suggest that PGA-2 and PGA-4 may suppress cytokines and cytotoxic mediators. Alternatively primary rat cortical neuronal cells (PRCN) can be used to evaluate the effects of PGA.

EXAMPLE 13

Evaluation of the *in-vivo* efficacy of PGA in a transgenic mouse model of AD.

Selection of Animal Model: The R1.40 *APP YAC* transgenic mice created by introducing entire genomic copies of mutant human APP (with K670N/M671L FAD substitutions) into the mouse genome can be utilized in the instant example. As compared to the cDNA based hAPP transgenic mice, the R1.40 *APP YAC* transgenic mice exhibit regional Aβ distribution, preferential deposition of $A\beta_{1-42}$, overlapping deposition of APOE, extensive neuritic abnormalities, and increased markers of inflammation mimicking many

characteristics of human AD. Inhibition of NF-κB by tolfenamic acid has been shown to reduce cerebral Aβ plaque burden in homozygous R1.40 mice.

Experimental procedures:

Animals: Starter pair of R1.40 [B6.129-Tg(APPSw)40Btla/Mmjax mice (Stock# 034831)] can be purchased from Jackson Laboratory (Bar Harbor, ME). Breeding colonies can be genotyped and maintained under standard animal housing conditions in a 12-hour dark light cycle with free access to food and water at the laboratory animal resource facility (LARC) at IU School of Medicine (IUSM). The background strain for R1.40 is mixed, which can serve as non-AD controls. All experiments can be conducted according to the Institutional Animal Care and Use Committee (IACUC) and approved by the local ethics committee.

PGA dosing and treatment regimen: The LD_{50} calculated using the in-vitro IC_{50} values and the regression equation [log (LD_{50}) =0.506xlog (IC_{50})+0.47551] for PGA-2 and PGA-4 equals 1396.83 mg/kg and 1693.87 mg/kg bodyweight respectively. Appropriate dose of PGA-2 and PGA-4 can be dissolved in 100µl of sterile PBS for i.p administration. R1.40 *APP YAC* transgenic mice develop parenchymal and vascular amyloid deposits by 12-13 months and exhibit reactive gliosis by 14-16 months. Four groups with 7 homozygous mutant *APP YAC* transgenic mice each can be administered daily either saline, PGA-2, PGA-4 or carrier peptide (TAT) at 1300 mg/kg (equivalent to LD_{50} of PGA-2) for four weeks beginning at week 40.

Histology: Mice can be perfused transcardially with ice cold PBS 4% paraformaldehyde at the end of four weeks. Brain tissues can be harvested, frozen and stored for histological analysis. Sections of entorhinal cortex, orbitofrontal cortex, and frontal cortex can be stained for congophilic dense-core amyloid plaques and immunostained for Aβ plaques and inflammatory markers including Iba1, IL-6, IL-1β, TNF-α, and NF-κB-p65.

Photomicrographs can be analyzed for percent stained area for plaque load and inflammation. An inflammatory focus is defined as the presence of clusters of 20 or more aggregated mononuclear cells. The total number of inflammatory foci can be counted from 3 different sections of each specimen.

Leuprolide (5g/kg) and glatiramer acetate (230mg/kg) administered i.p. for similar periods were efficacious in models of AD. These peptides have been measured in the cerebrospinal fluid in optimum concentrations suggesting efficient CNS delivery and substantiating the credibility of peptide drugs for AD. Based on the mechanisms of actions of

GILZ and preliminary data, percent stained area of congo red positive plaques, Aβ plaques and inflammation may be significantly reduced in PGA treated mice.

EXAMPLE 14

Transformation of PGA into small molecule agents: PGA peptides are rationally designed structural mimics of GILZ in the contest of the p65-TAD binding interface. Specific inhibition of activated p65 by PGA has been shown to suppress inflammatory and cytotoxic responses *in-vitro* and *in-vivo.*

Three dimensional structure databases incorporated within the modeling programs of CAVEAT and PHASE can be searched to identify templates with bonds that adopt PP_{II} orientation and serve as attachment points. The functional groups of critical proline of human GILZ or the substituted PGA residue can be grafted onto the non-peptide scaffold. The resultant PGA pharmacophore can be characterized by binding affinity and functional studies. A similar approach has been previously used successfully in developing inhibitors of Factor Xa for treating coagulation pathologies.

PepMMsMIMIC is a virtual screening platform tool used to identify pharmacophore or chemical compounds that mimic a natural peptide or protein in 3D space. Using this tool, a three dimensional similarity search of PGA-2/PGA-4 structure can be initiated amongst seventeen million conformers calculated from commercially available chemicals. Top peptide mimetic can be ranked by two different scoring functions taking into account high electrostatic, chemical and shape complementarity together with pharmacophore fingerprints similarity. Using this method, multiple small molecule nutlin analogues have been identified as peptidomimetics of MDM2/p53 interaction. Preliminary search suggests that the chemical moiety, methyl-N-butyl-N [2,6-di-nitro-4-(trifluormethyl)phenyl] carbamate, may be similar to PGA-2 peptide.

Modified amino acids or incorporation of enantiomers may be used to enhance identification of PGA specific pharmacophore.

CLAIMS

1. A pharmaceutical composition comprising a polypeptide from about 8 to about 12 amino acid residues, the polypeptide comprising a tetrapeptide having the sequence of PXXP, wherein

P is proline; and

X is any amino acid.

2. The pharmaceutical composition of claim 1, wherein the polypeptide comprises a sequence of Formula I: X1-X2-X3-P-X4-X5-P-X6-X7,

wherein each of X1, X2, X3, X4, X5, X6, and X7 is independently any amino acid.

3. The pharmaceutical composition of claim 1, wherein the polypeptide comprises a sequence of XXXPXXPXX.

4. The pharmaceutical composition of claim 3, wherein the polypeptide comprises a sequence of EPAPXXPXX (SEQ ID NO: 1).

5. The pharmaceutical composition of claim 3, wherein the polypeptide comprises a sequence of EPLPXXPXX (SEQ ID NO: 2).

6. The pharmaceutical composition of claim 3, wherein the polypeptide comprises a sequence of EAAPXXPXX (SEQ ID NO: 3).

7. The pharmaceutical composition of claim 3, wherein the polypeptide comprises a sequence of APAPXXPXX (SEQ ID NO: 4).

8. The pharmaceutical composition of claim 3, wherein the polypeptide comprises a sequence of APKPXXPXX (SEQ ID NO: 5).

9. The pharmaceutical composition of claim 1, wherein the polypeptide comprises a sequence of Formula II: X1-X2-X3-P-X4-X5-P-X6-X7-X8,

wherein each of X1, X2, X3, X4, X5, X6, X7, and X8 is independently any amino acid.

10. The pharmaceutical composition of claim 1, wherein the polypeptide comprises a sequence of XXXPXXPXXX.

11. The pharmaceutical composition of claim 10, wherein the polypeptide comprises a sequence of EPAPXXPXXX (SEQ ID NO: 6).

12. The pharmaceutical composition of claim 10, wherein the polypeptide comprises a sequence of EPLPXXPXXX (SEQ ID NO: 7).

13. The pharmaceutical composition of claim 10, wherein the polypeptide comprises a sequence of EAAPXXPXXX (SEQ ID NO: 8).

14. The pharmaceutical composition of claim 10, wherein the polypeptide comprises a sequence of APAPXXPXXX (SEQ ID NO: 9).

15. The pharmaceutical composition of claim 10, wherein the polypeptide comprises a sequence of APKPXXPXXX (SEQ ID NO: 10).

16. The pharmaceutical composition of claim 1, wherein the polypeptide comprises a sequence of EPAPRQPAT (SEQ ID NO: 11).

17. The pharmaceutical composition of claim 1, wherein the polypeptide comprises a sequence of EPAPRAPEG (SEQ ID NO: 12).

18. The pharmaceutical composition of claim 1, wherein the polypeptide comprises a sequence of EPAPLAPYG (SEQ ID NO: 13).

19. The pharmaceutical composition of claim 1, wherein the polypeptide comprises a sequence of EPAPRAPGT (SEQ ID NO: 14).

20. The pharmaceutical composition of claim 1, wherein the polypeptide comprises a sequence of EPAPRAPDG (SEQ ID NO: 15).

21. The pharmaceutical composition of claim 1, wherein the polypeptide comprises a sequence of EPLPEAPDT (SEQ ID NO: 16).

22. The pharmaceutical composition of claim 1, wherein the polypeptide comprises a sequence of EPAPESPQV (SEQ ID NO: 17).

23. The pharmaceutical composition of claim 1, wherein the polypeptide comprises a sequence of EPAPEQPDG (SEQ ID NO: 18).

24. The pharmaceutical composition of claim 1, wherein the polypeptide comprises a sequence of APAPASPQV (SEQ ID NO: 19).

25. The pharmaceutical composition of claim 1, wherein the polypeptide comprises a sequence of EAAAESPQV (SEQ ID NO: 20).

26. The pharmaceutical composition of claim 1, wherein the polypeptide comprises a sequence of APAPAAPET (SEQ ID NO: 21).

27. The pharmaceutical composition of claim 1, wherein the polypeptide comprises a sequence of EAAAEAAET (SEQ ID NO: 22).

28. The pharmaceutical composition of claim 1, wherein the polypeptide comprises a sequence of EPAPEAPEGY (SEQ ID NO: 23).

29. The pharmaceutical composition of claim 1, wherein the polypeptide comprises a sequence of EPAPYQPEG (SEQ ID NO: 24).

30. The pharmaceutical composition of claim 1, wherein the polypeptide comprises a sequence of EPAYEAQET (SEQ ID NO: 25).

31. The pharmaceutical composition of claim 1, wherein the polypeptide comprises a sequence of EPAPEAGET (SEQ ID NO: 26).

32. The pharmaceutical composition of claim 1, wherein the polypeptide comprises a sequence of EPAPEAPET (SEQ ID NO: 27).

33. The pharmaceutical composition of claim 1, wherein the composition suppresses p65 binding.

34. The pharmaceutical composition of claim 1, wherein the composition suppresses p65 activation.

35. The pharmaceutical composition of claim 1, wherein the composition inhibits NF-κB translocation to the nucleus of a cell.

36. A pharmaceutical formulation comprising the pharmaceutical composition of claim 1.

37. The pharmaceutical formulation of claim 36 further comprising a pharmaceutically acceptable carrier.

38. The pharmaceutical formulation of claim 36 optionally including one or more other therapeutic ingredients.

39. The pharmaceutical formulation of claim 36 wherein the formulation is a single unit dose.

40. A lyophilisate or powder of the pharmaceutical formulation of claim 39.

41. An aqueous solution produced by dissolving the lyophilisate or powder of claim 40 in water.

42. Use of the pharmaceutical composition of claim 1 for the treatment of a neurodegenerative disease in a patient.

43. The use of claim 42 wherein the neurodegenerative disease is Alzheimer's Disease.

44. The use of claim 42 wherein the neurodegenerative disease is Parkinson's Disease.

45. The use of claim 42 wherein the neurodegenerative disease is multiple sclerosis.

46. The use of claim 42 wherein the neurodegenerative disease is amyotrophic lateral sclerosis (ALS).

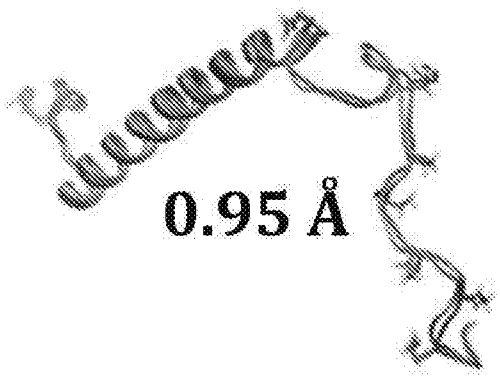

FIG. 1A

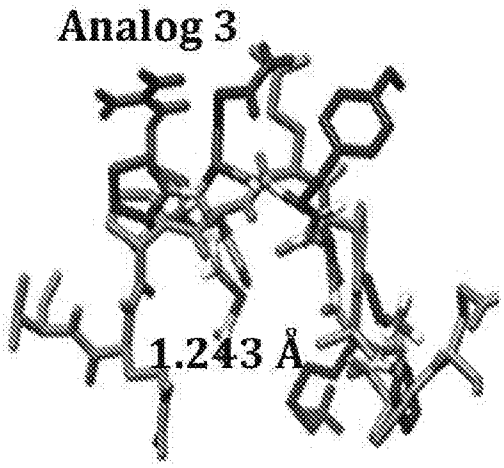

FIG. 1B

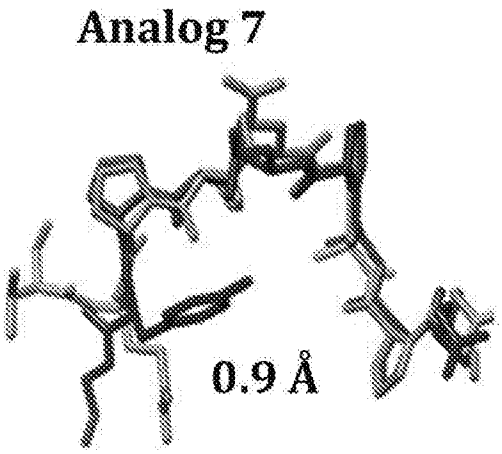

FIG. 1C

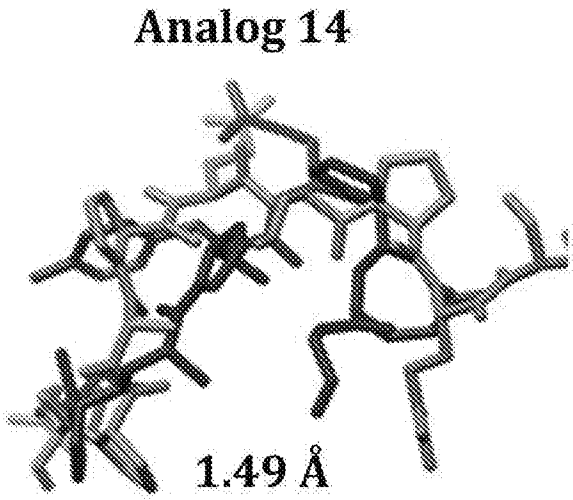

FIG. 1D

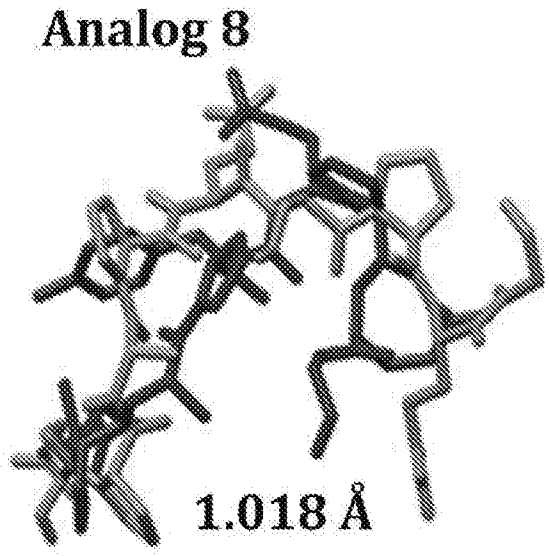

FIG. 1E

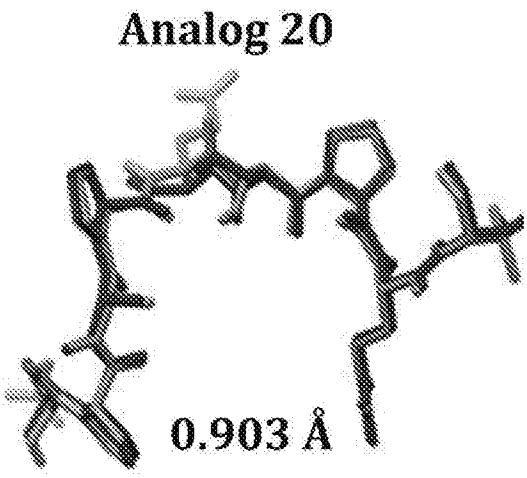

FIG. 1F

p65: Wild type GILZ-P

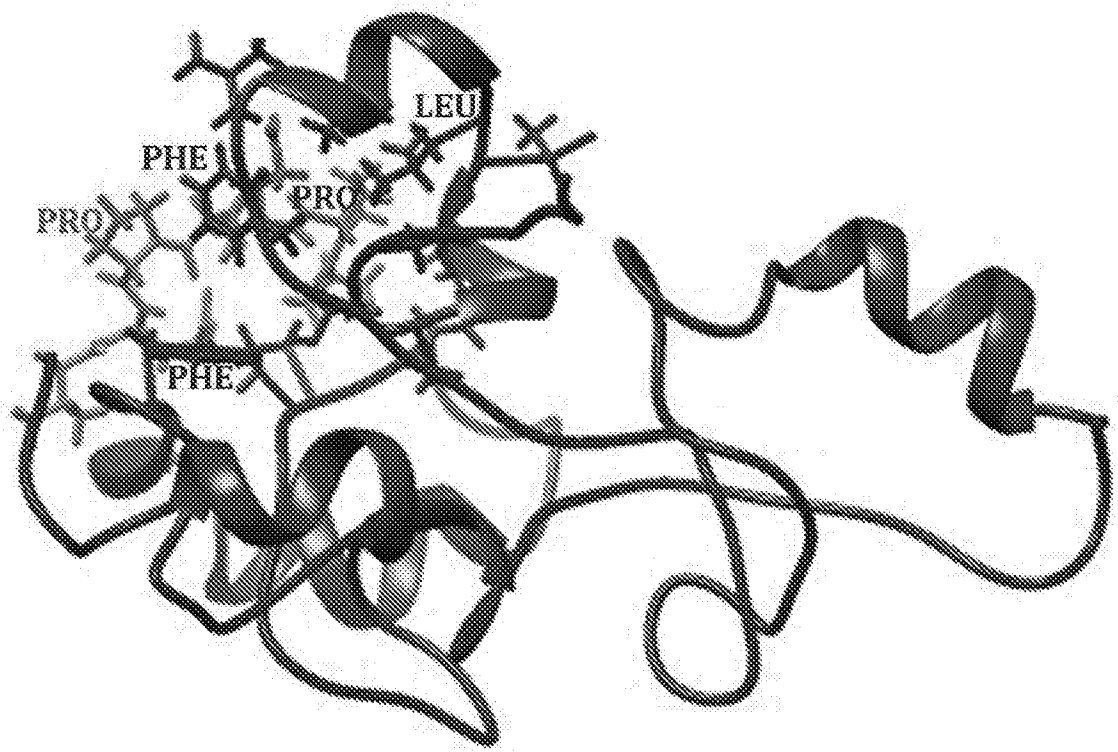

FIG. 2A

p65: Analog 3

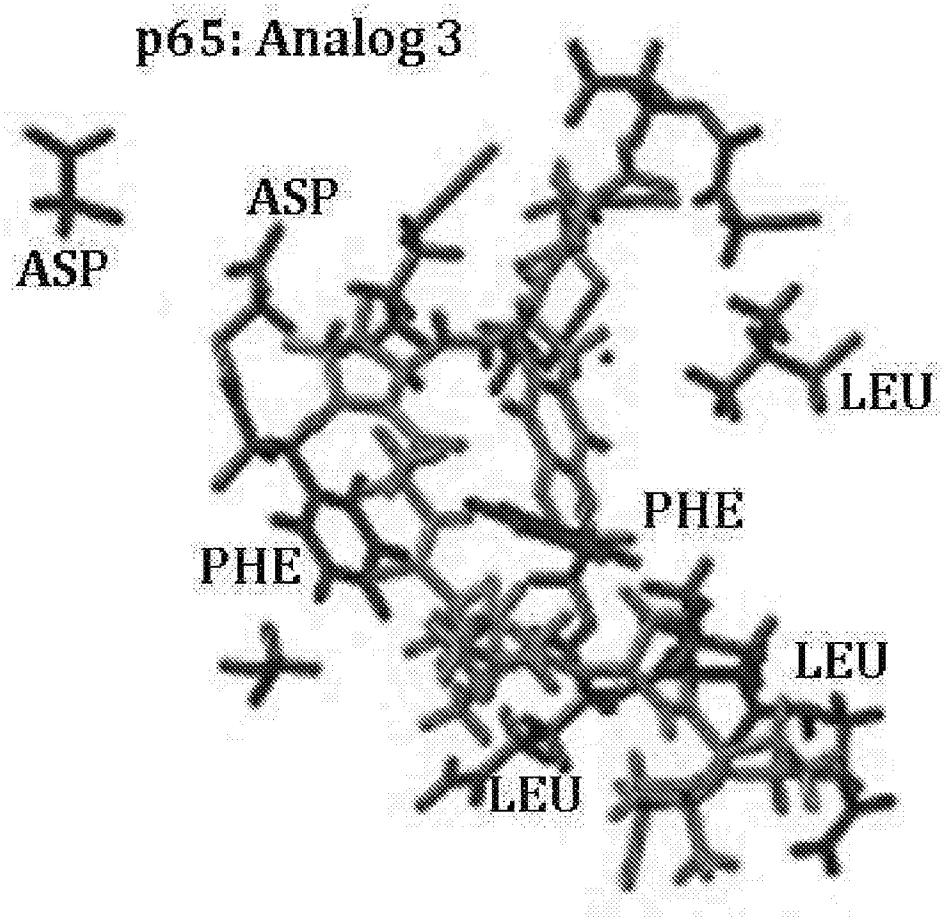

FIG. 2B

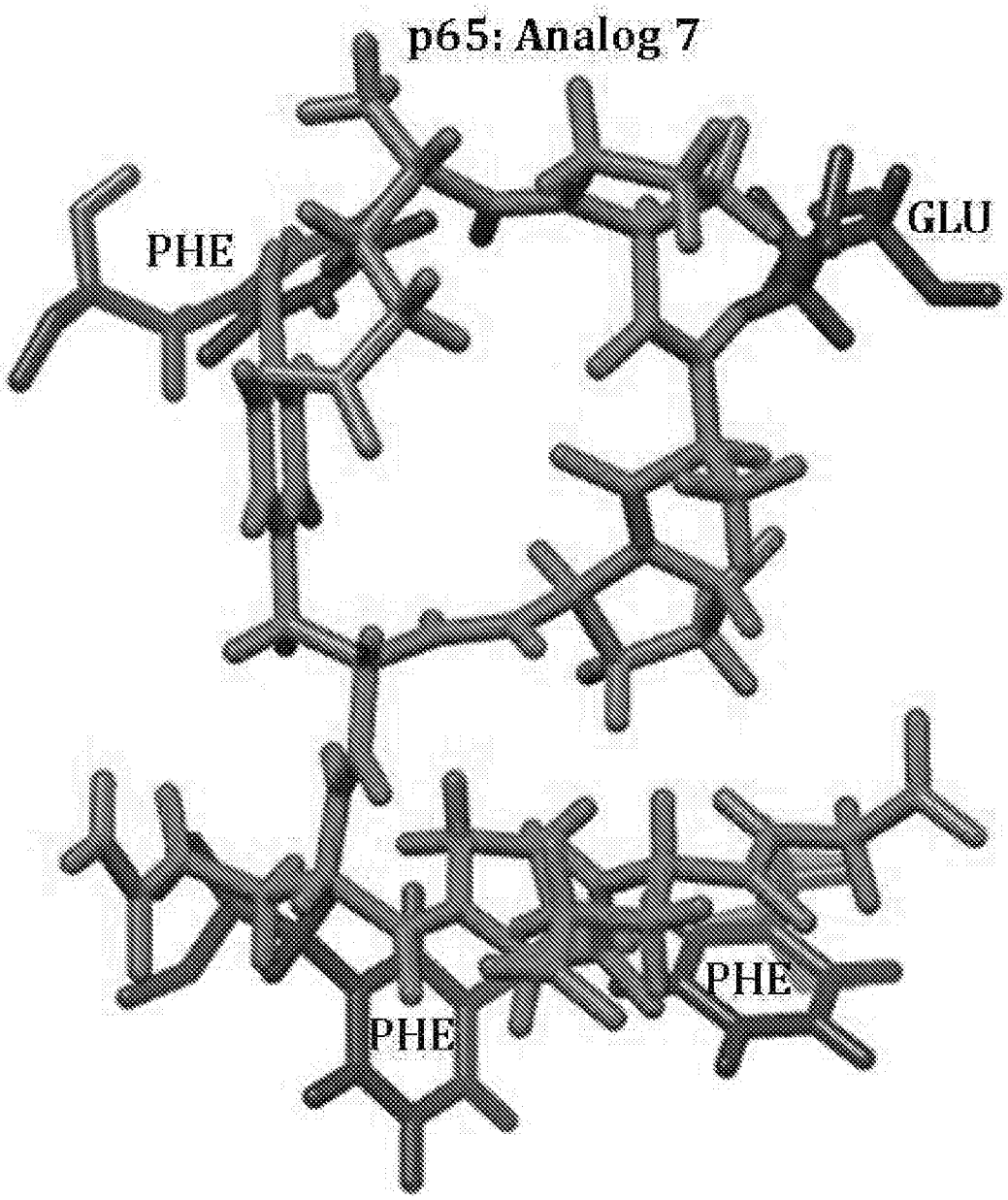

FIG. 2C

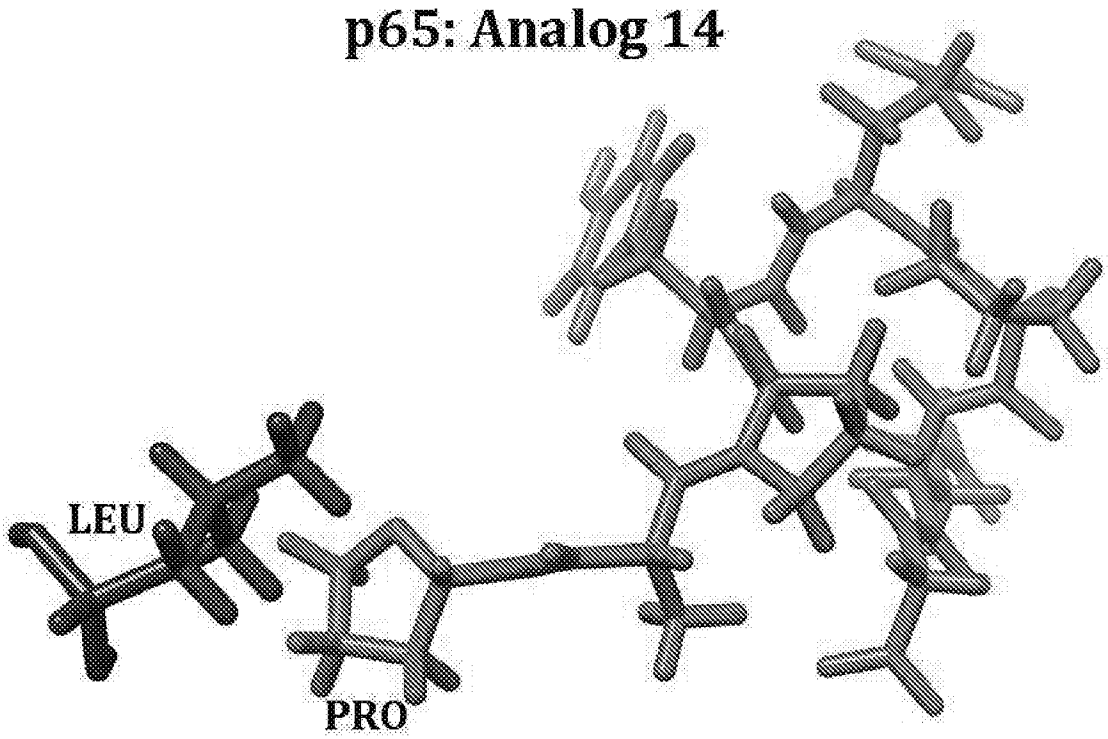

FIG. 2D

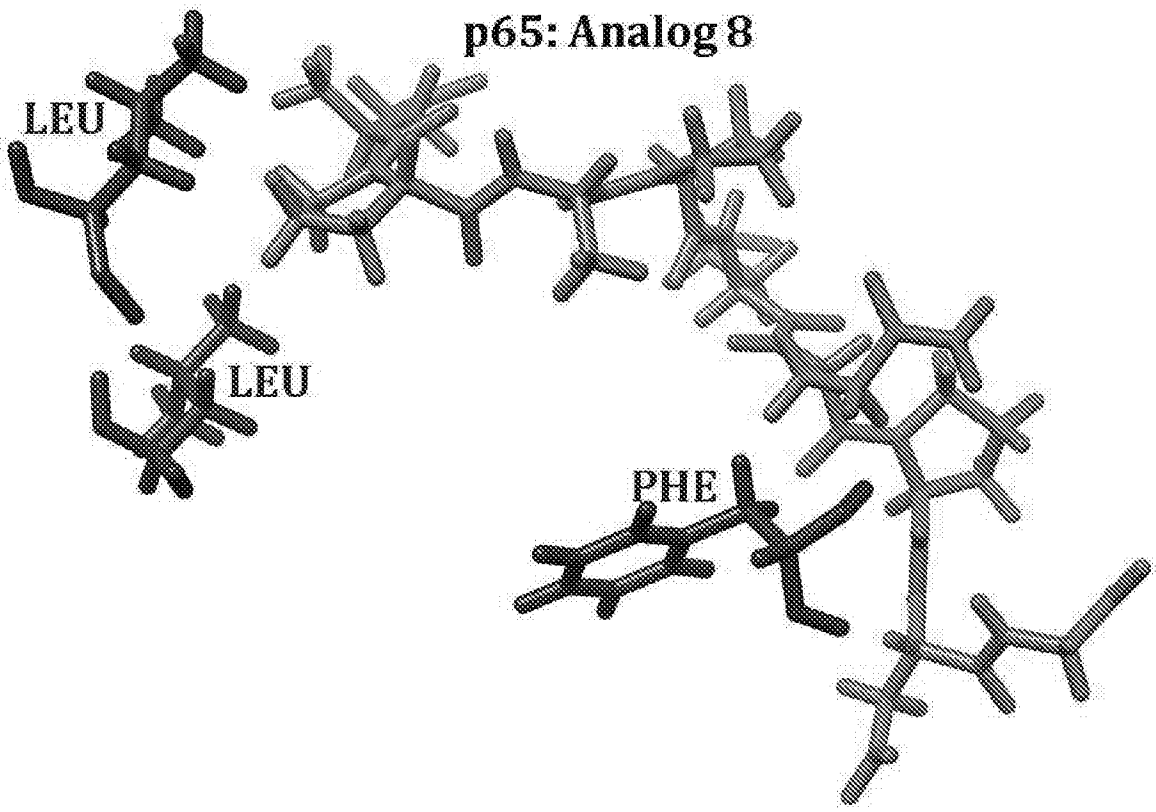

FIG. 2E

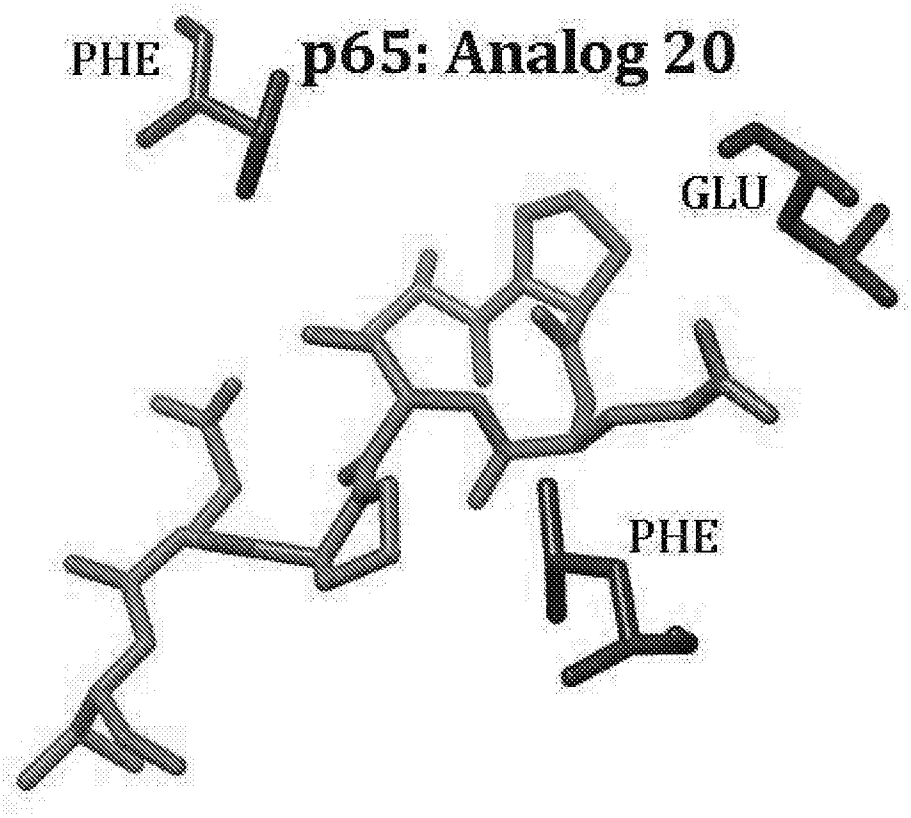

FIG. 2F

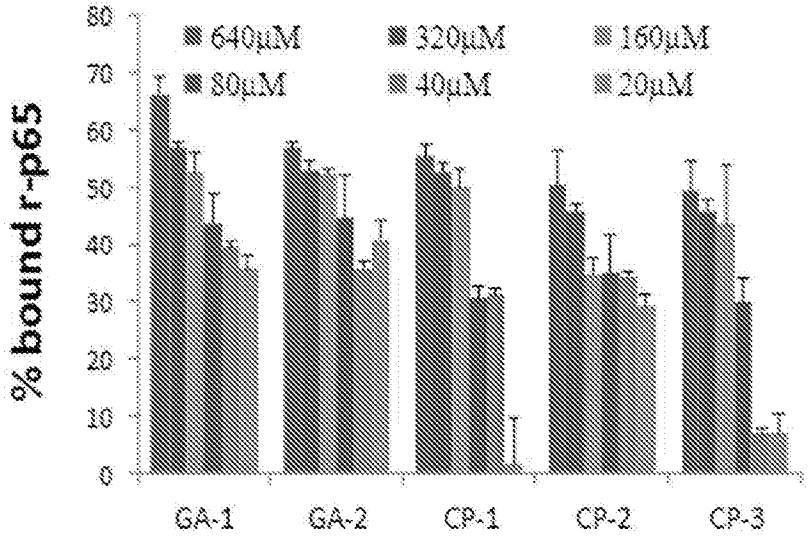
% bound r-p65
640μM
320μM
160μM
80μM
40μM
20μM
0
10
20
30
40
50
60
70
80
GA-1
GA-2
CP-1
CP-2
CP-3

FIG. 3A

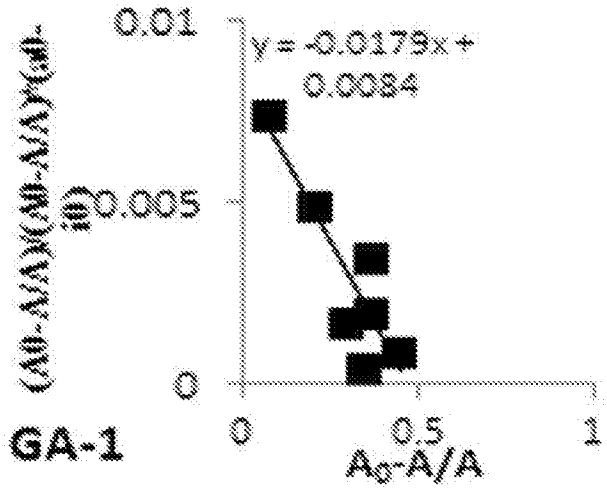
y = -0.0179x + 0.0084
0.01
0.005
0
0
0.5
1
GA-1
A0-A/A

FIG. 3B

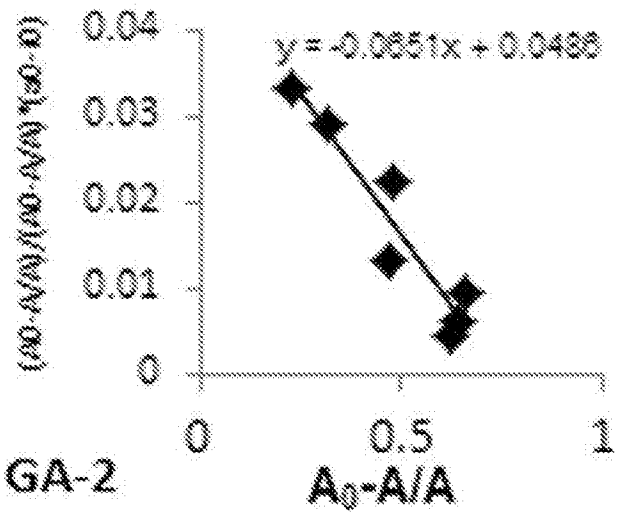
y = -0.0851x + 0.0488
0.04
0.03
0.02
0.01
0
0
0.5
1
GA-2
A0-A/A

FIG. 3C

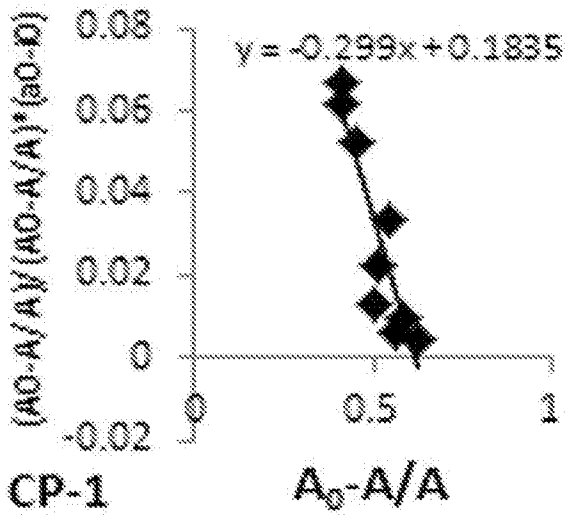
y = -0.299x + 0.1835
0.08
0.06
0.04
0.02
0
-0.02
0
0.5
1
CP-1
A0-A/A

FIG. 3D

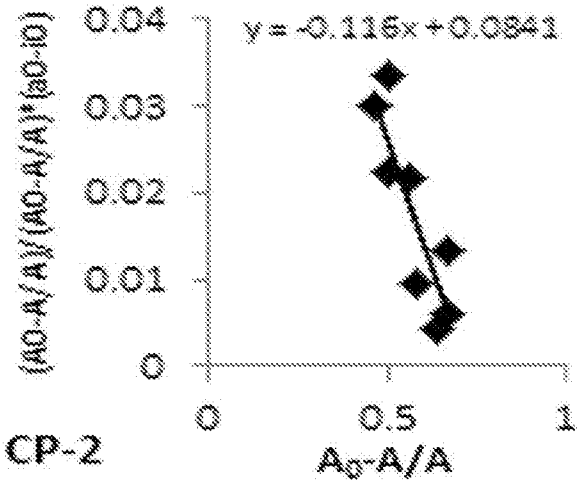
y = -0.116x + 0.0841
0.04
0.03
0.02
0.01
0
0
0.5
1
(A0-A/A)/(A0-A/A)*(a0-i0)
A0-A/A
CP-2

FIG. 3E

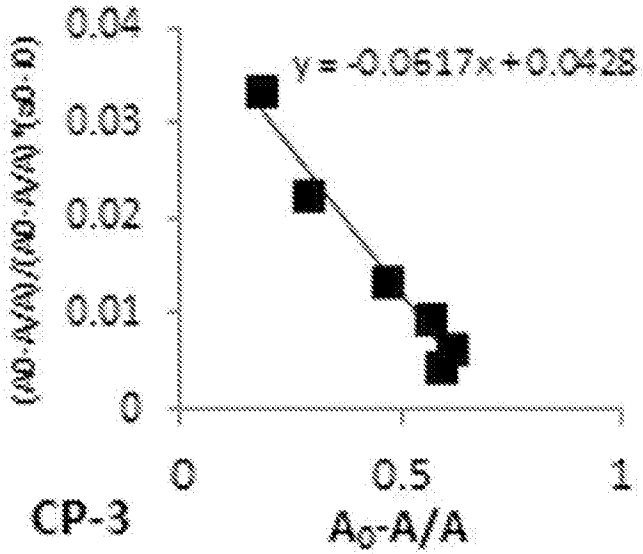
y = -0.0617x + 0.0428
0.04
0.03
0.02
0.01
0
0
0.5
1
(A0-A/A)/(A0-A/A)*(a0-i0)
A0-A/A
CP-3

FIG. 3F

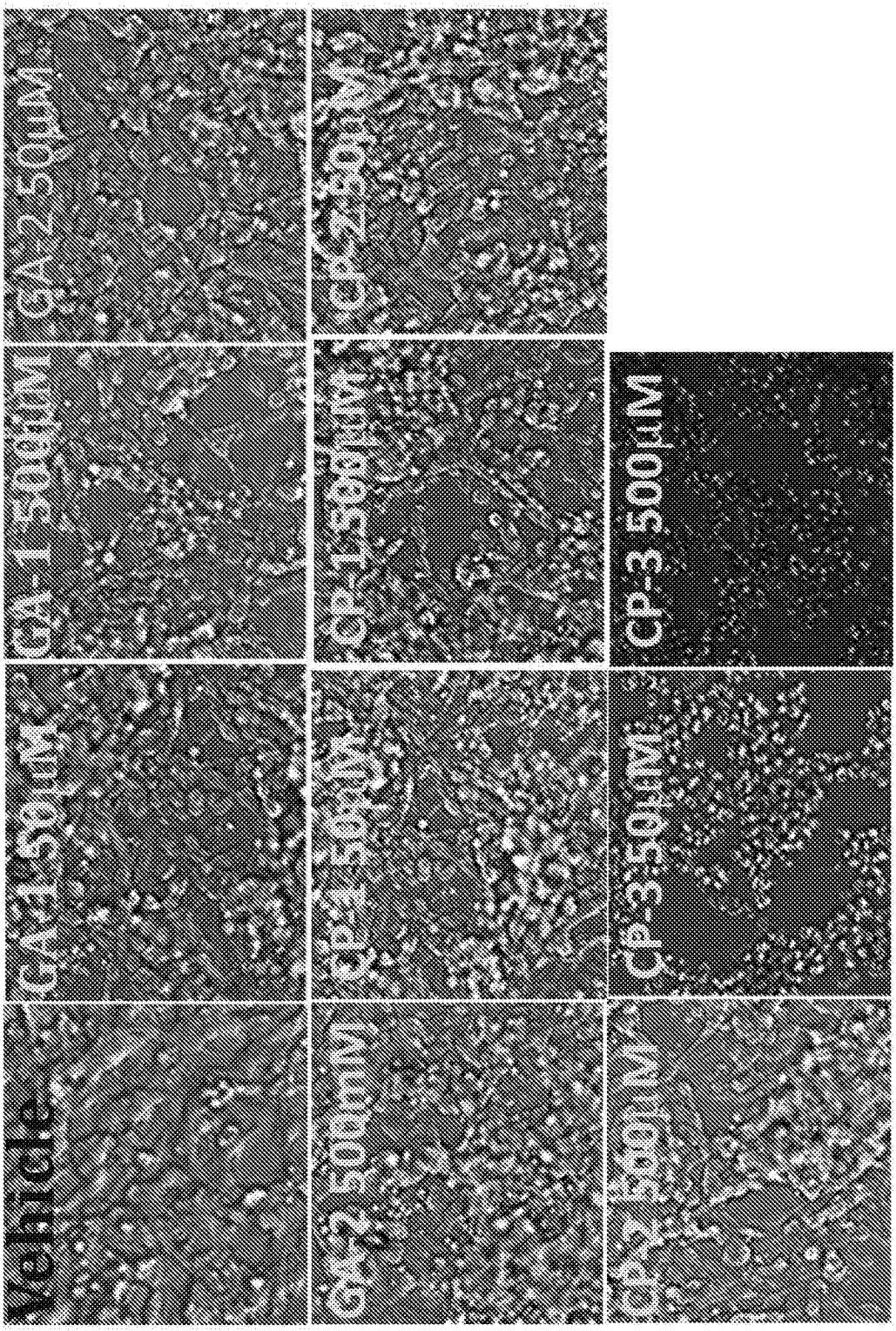
Vehicle
GA-1 500μM
GA-2 500μM
GA-3 500μM
GA-1 500μM + GA-2 500μM
GA-2 500μM + GA-3 500μM
CP-1 500μM
CP-2 500μM
CP-3 500μM
CP-1 500μM + CP-2 500μM
CP-2 500μM + CP-3 500μM

FIG. 4A

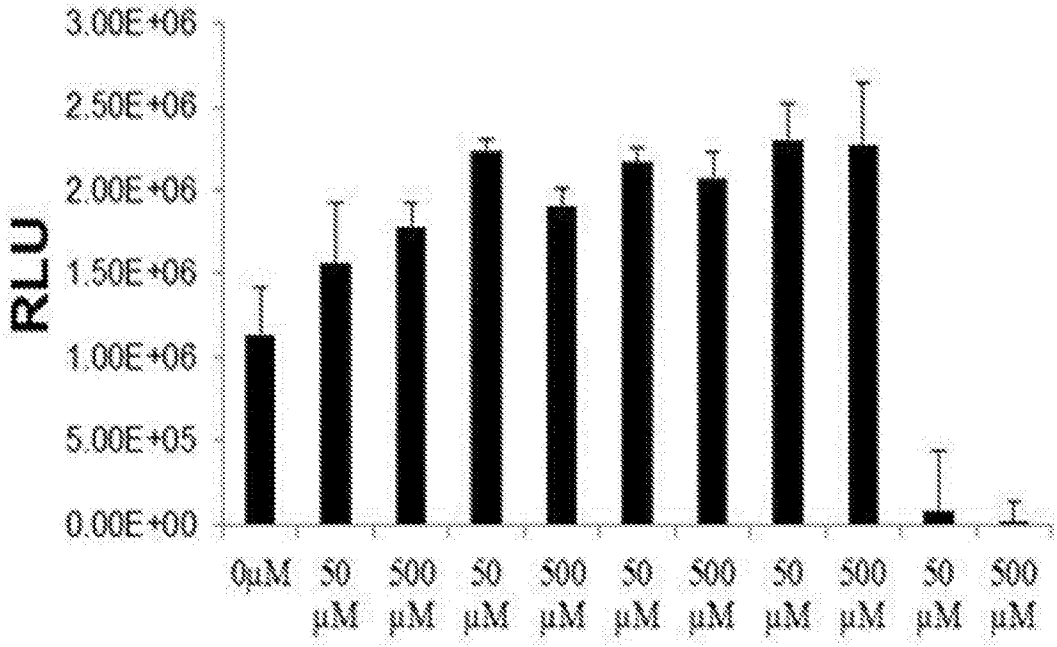
RLU
3.00E+06
2.50E+06
2.00E+06
1.50E+06
1.00E+06
5.00E+05
0.00E+00
0μM
50 μM
500 μM
50 μM
500 μM
50 μM
500 μM
50 μM
500 μM
50 μM
500 μM

FIG. 4B

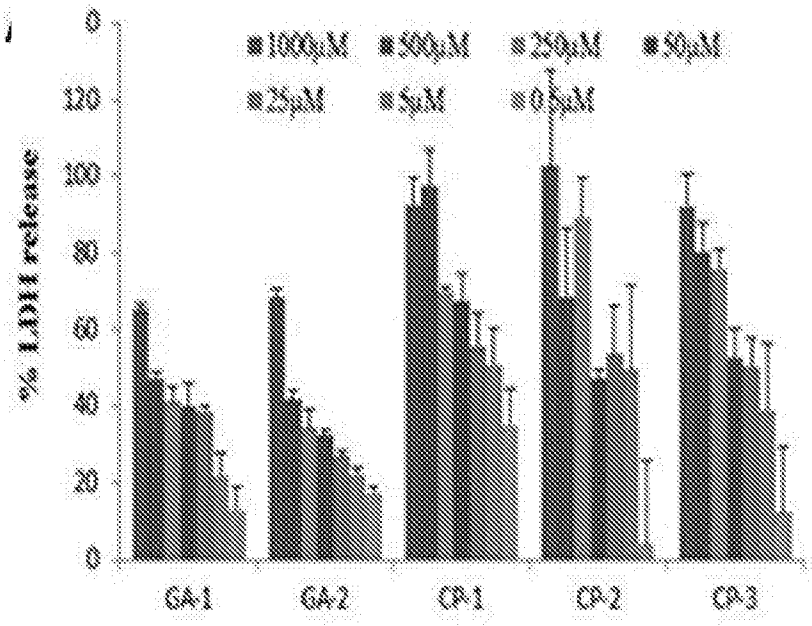
1000μM
500μM
250μM
50μM
25μM
5μM
0.5μM
% LDH release
0
20
40
60
80
100
120
GA-1
GA-2
CP-1
CP-2
CP-3

FIG. 5A

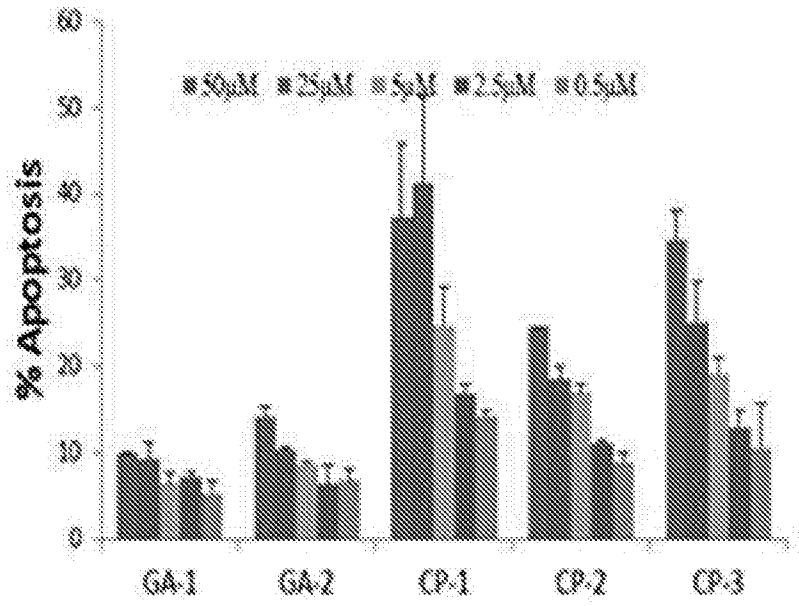
50μM
25μM
5μM
2.5μM
0.5μM
% Apoptosis
0
10
20
30
40
50
60
GA-1
GA-2
CP-1
CP-2
CP-3

FIG. 5B

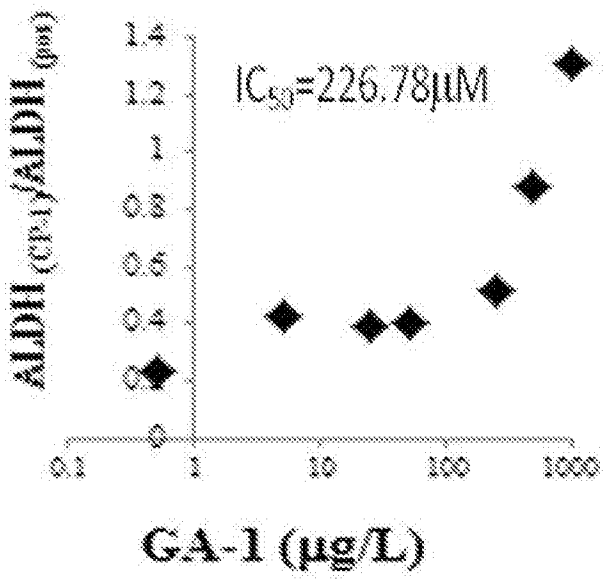
ALDH (CP-1)/ALDH (pos)
1.4
1.2
1
0.8
0.6
0.4
0
0.1
1
10
100
1000
IC50=226.78μM
GA-1 (μg/L)

FIG. 5C

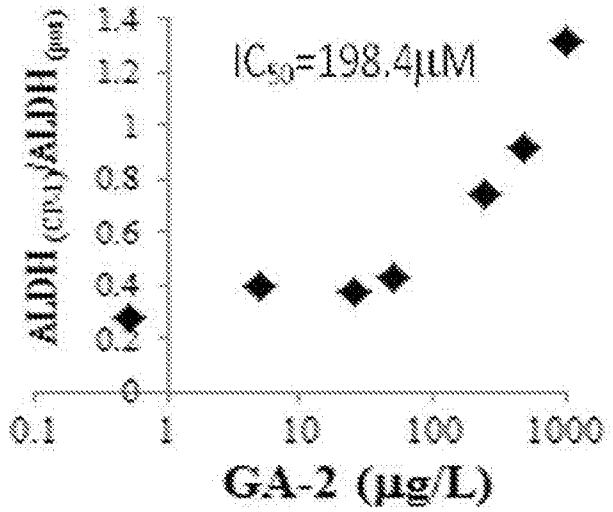
ALDH (CP-1)/ALDH (pos)
1.4
1.2
1
0.8
0.6
0.4
0.2
0
0.1
1
10
100
1000
IC50=198.4μM
GA-2 (μg/L)

FIG. 5D

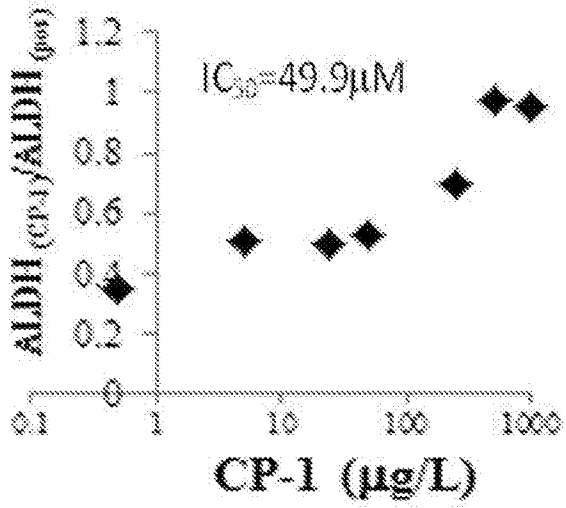
IC50=49.9μM
ALDH (CP-1)/ALDH (pre)
1.2
1
0.8
0.6
0.4
0.2
0
0.1
1
10
100
1000
CP-1 (μg/L)

FIG. 5E

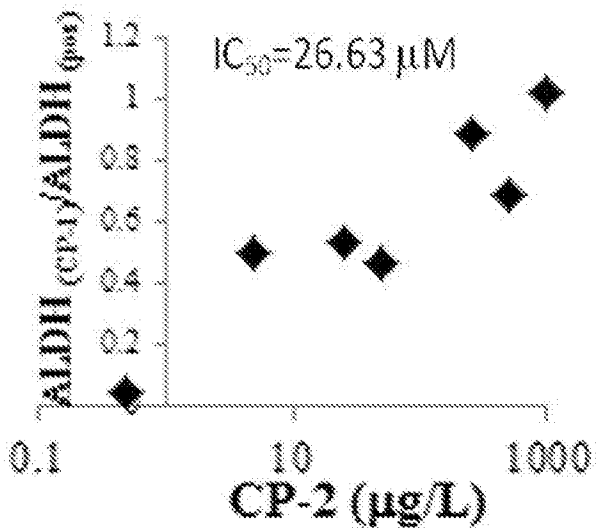
IC50=26.63 μM
ALDH (CP-1)/ALDH (pre)
1.2
1
0.8
0.6
0.4
0.2
0.1
10
1000
CP-2 (μg/L)

FIG. 5F

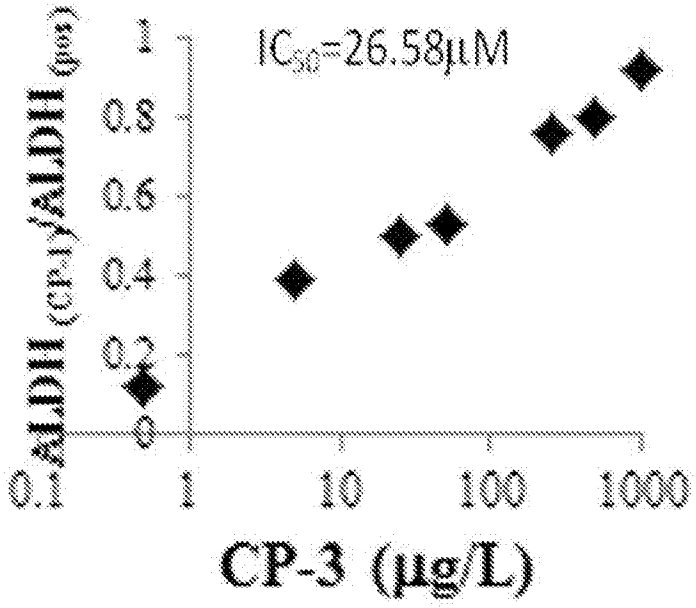

FIG. 5G

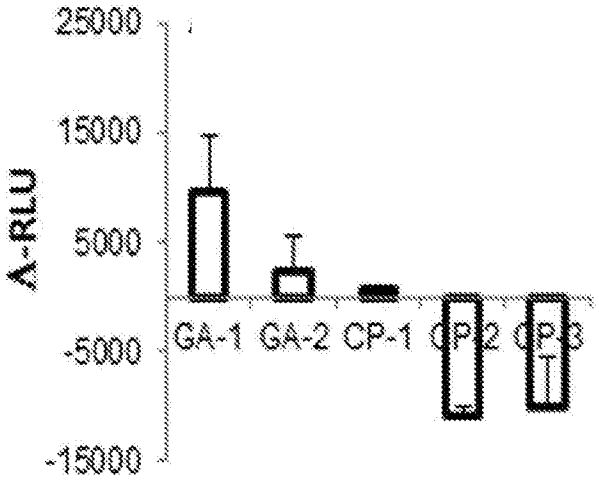
25000
15000
5000
-5000
-15000
A-RLU
GA-1
GA-2
CP-1

FIG. 6A

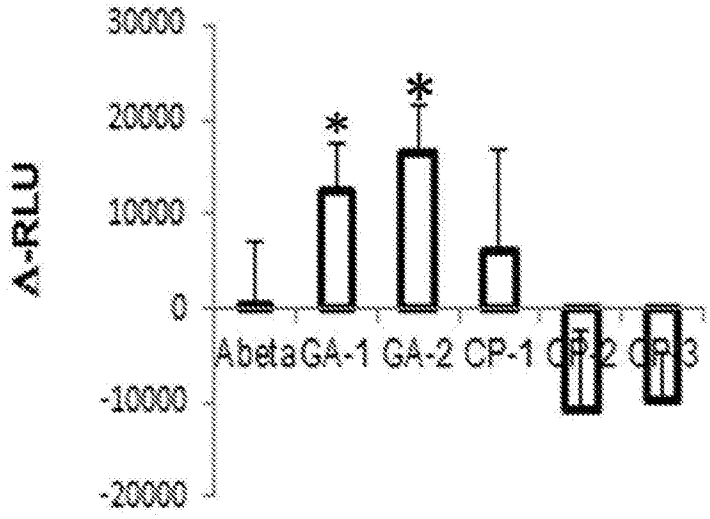
30000
20000
10000
0
-10000
-20000
A-RLU
*
*
Abeta
GA-1
GA-2
CP-1

FIG. 6B

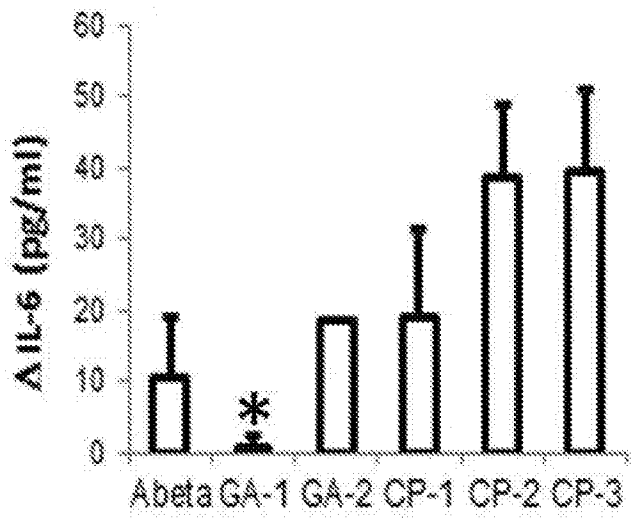
Δ IL-6 (pg/ml)
60
50
40
30
20
10
0
*
Abeta GA-1 GA-2 CP-1 CP-2 CP-3

FIG. 6C

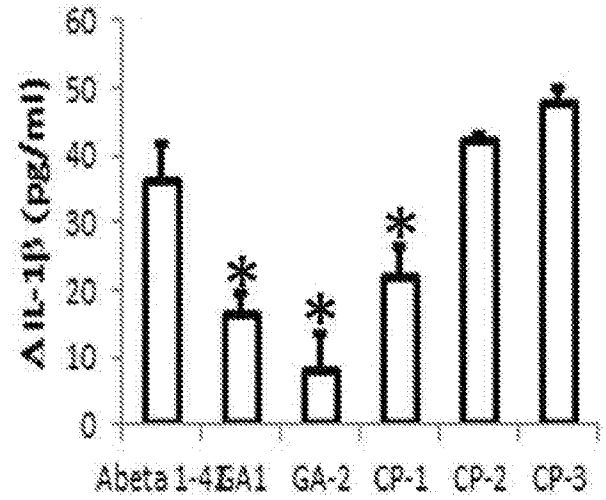
Δ IL-1β (pg/ml)
60
50
40
30
20
10
0
*
*
*
Abeta 1-4EA1 GA-2 CP-1 CP-2 CP-3

FIG. 6D

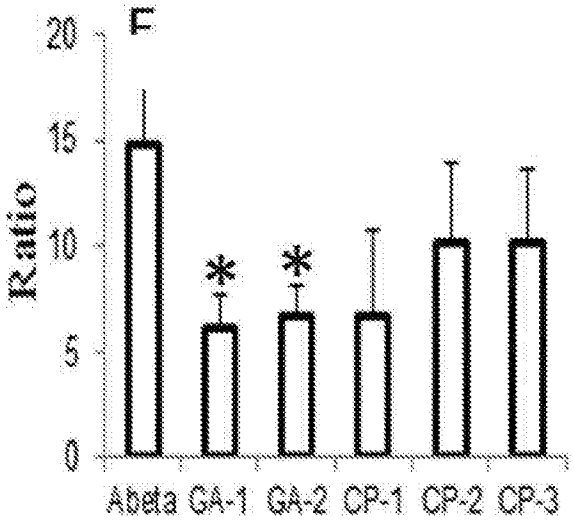

FIG. 6E

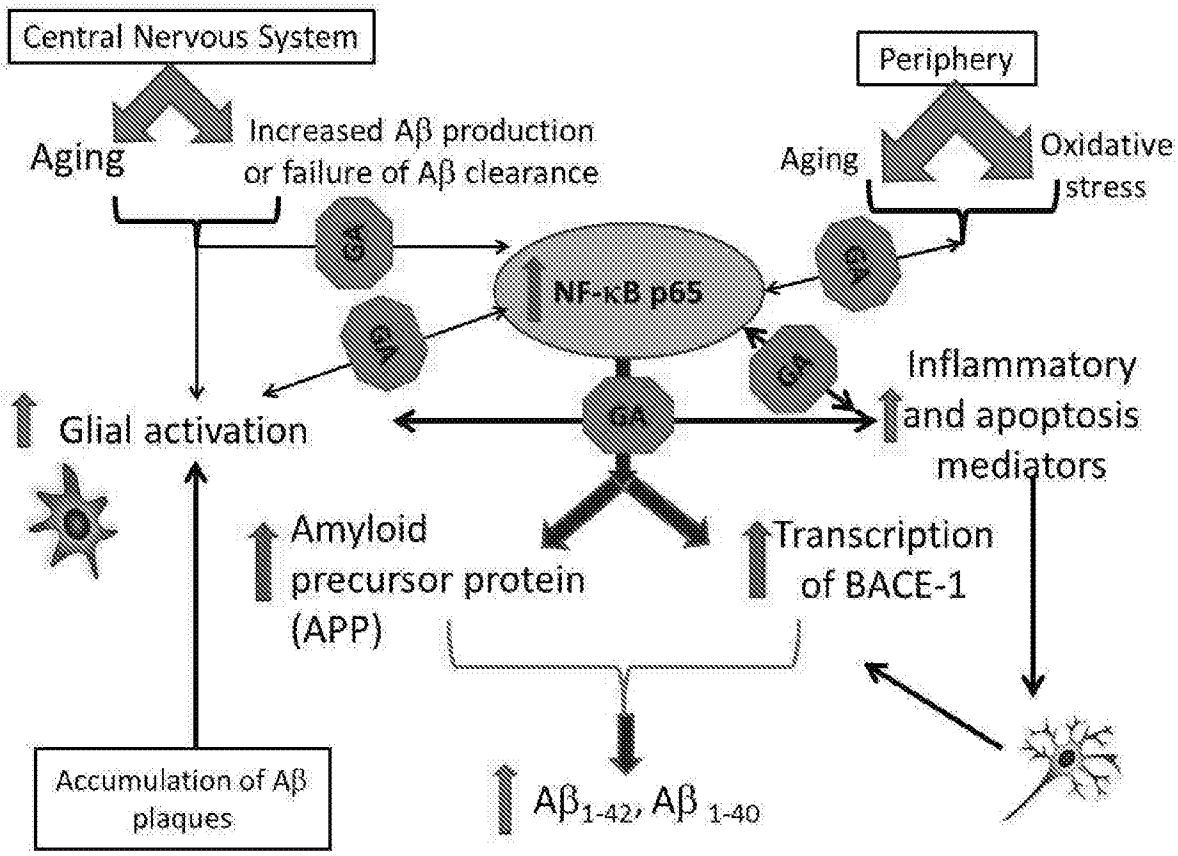
Central Nervous System
Periphery
Aging
Increased Aβ production or failure of Aβ clearance
Aging
Oxidative stress
CP
CP
CP
CP
NF-κB p65
GA
Glial activation
Inflammatory and apoptosis mediators
Amyloid precursor protein (APP)
Transcription of BACE-1
Accumulation of Aβ plaques
Aβ1-42, Aβ 1-40

FIG. 7

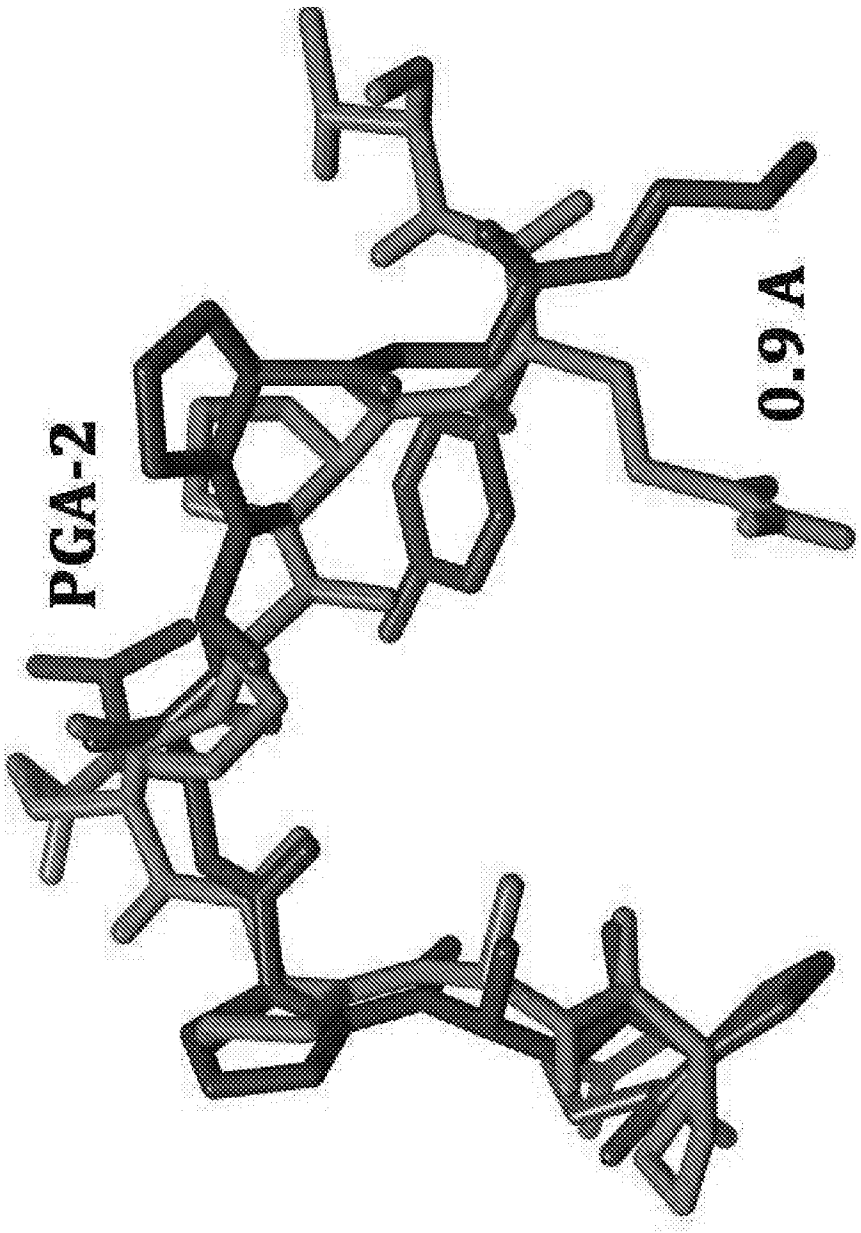

FIG. 8A

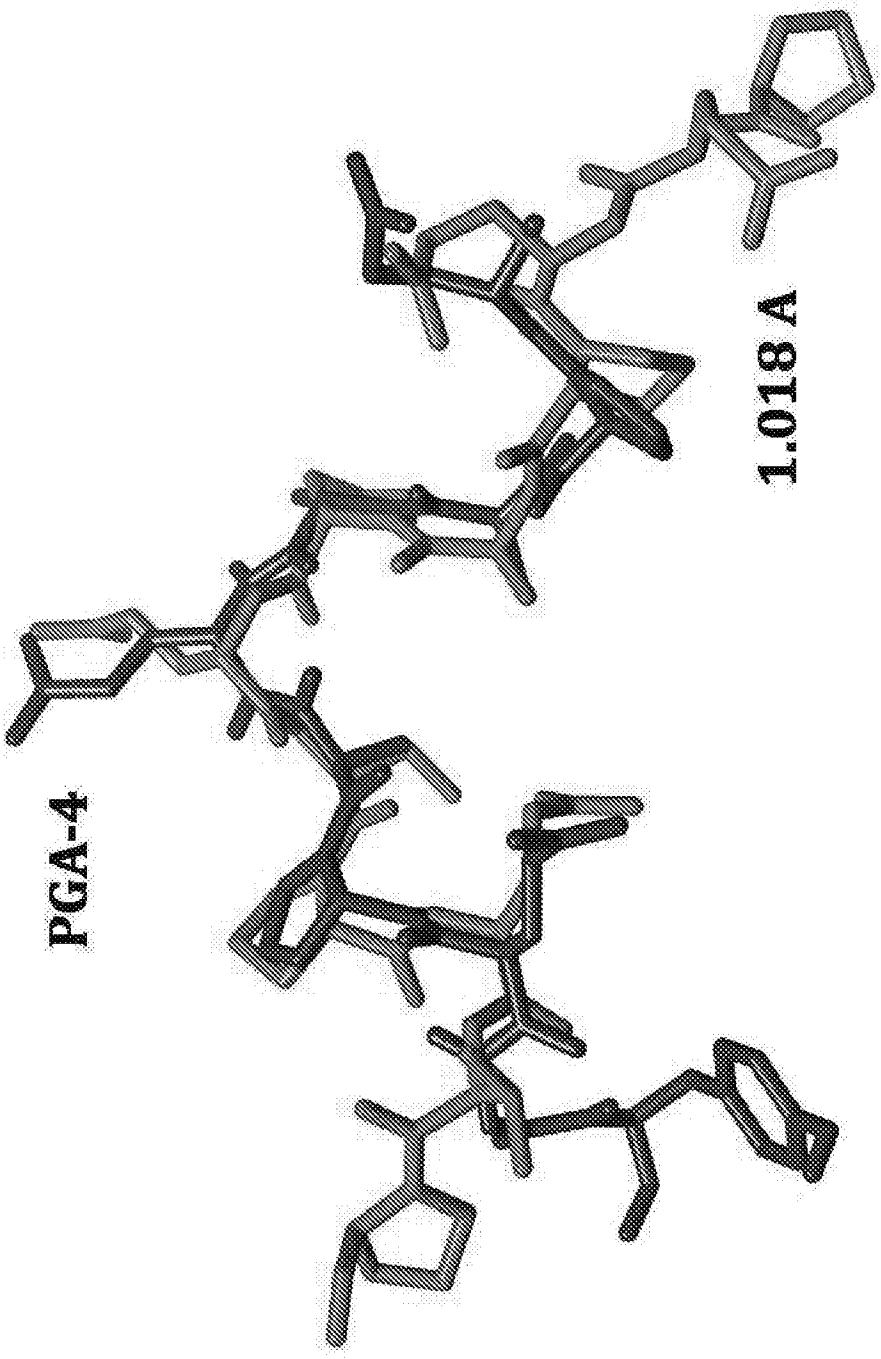

FIG. 8B

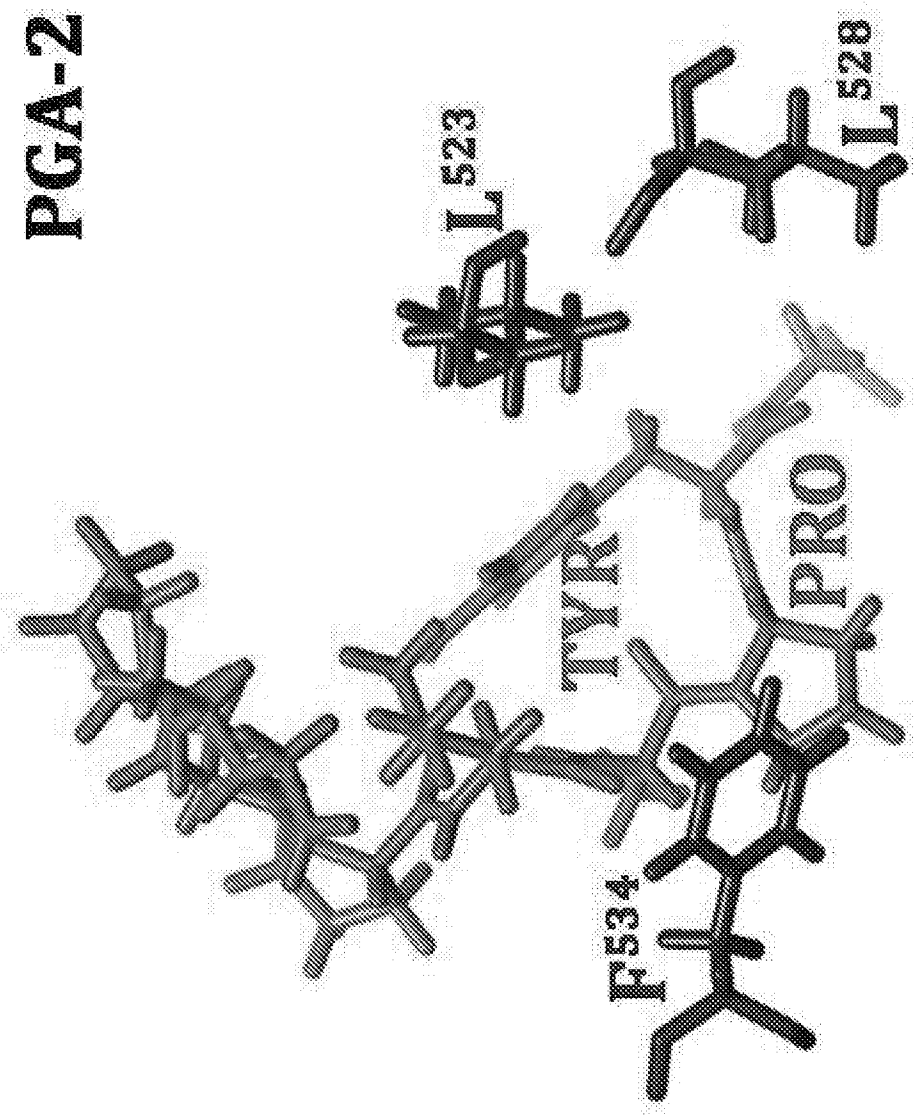

FIG. 8C

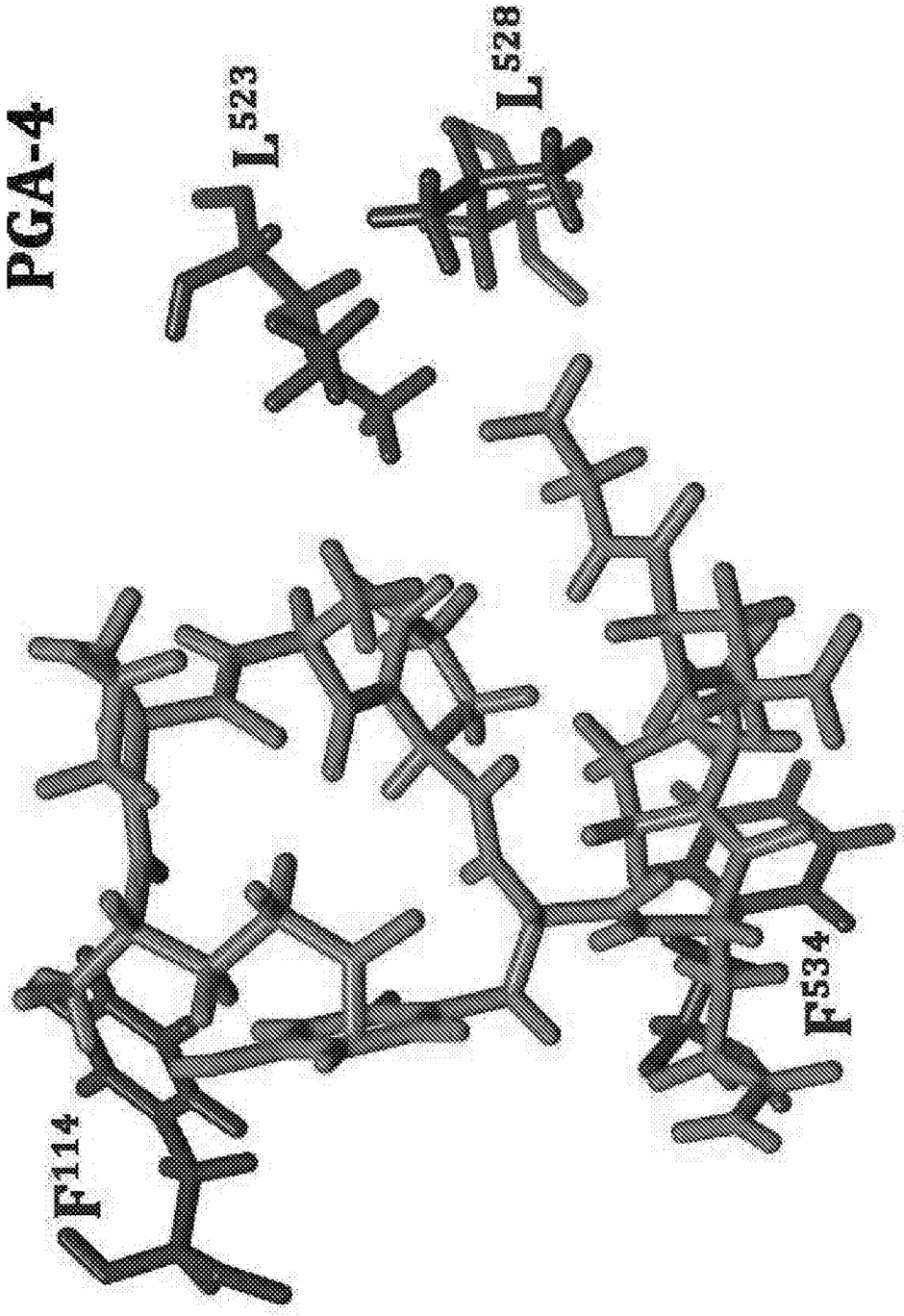

FIG. 8D

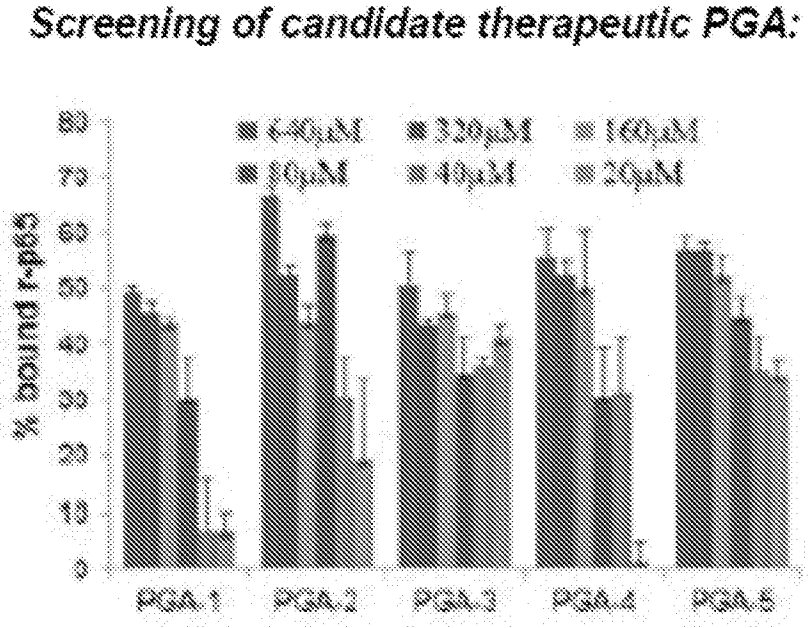
Screening of candidate therapeutic PGA:
% bound r-p53
80
70
60
50
40
30
20
10
0
640μM
320μM
160μM
80μM
40μM
20μM
PGA-1
PGA-2
PGA-3
PGA-4
PGA-5

FIG. 9A

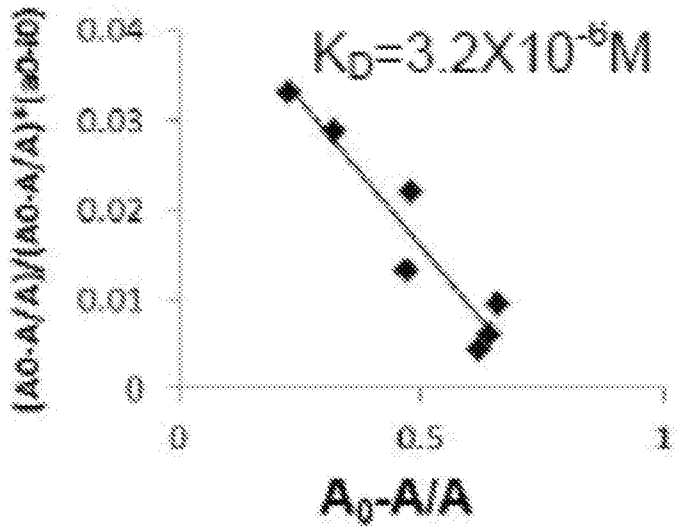
(A0-A/A)/(A0-A/A)*(=Δ0-Δ)
0.04
0.03
0.02
0.01
0
0
0.5
1
A0-A/A
KD=3.2X10-6M

FIG. 9B

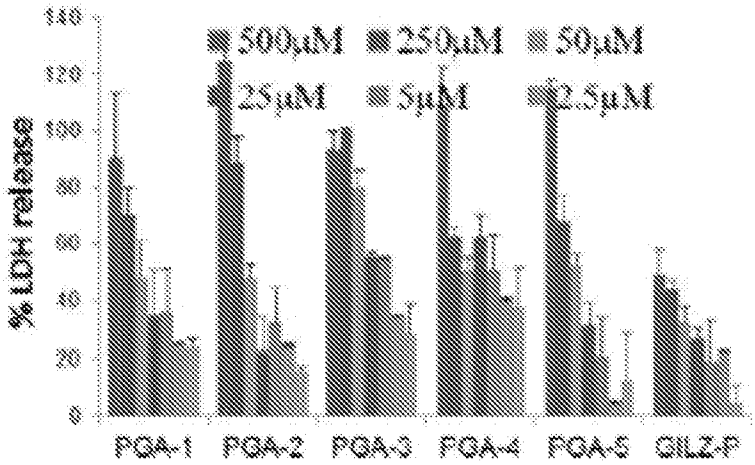

FIG. 10A

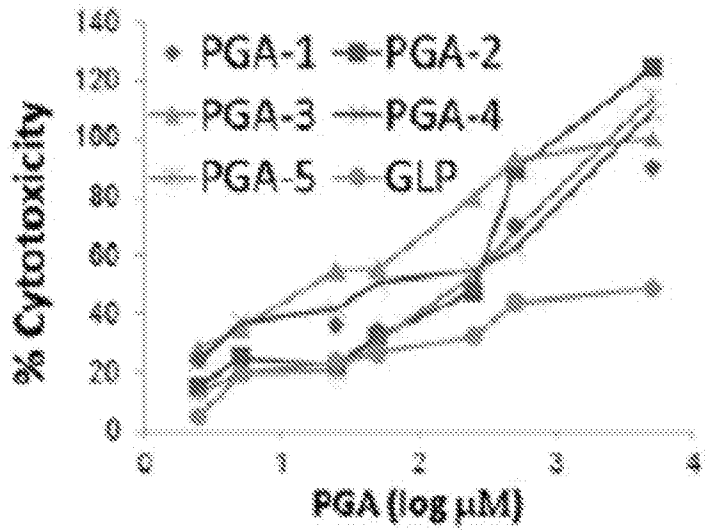

FIG. 10B

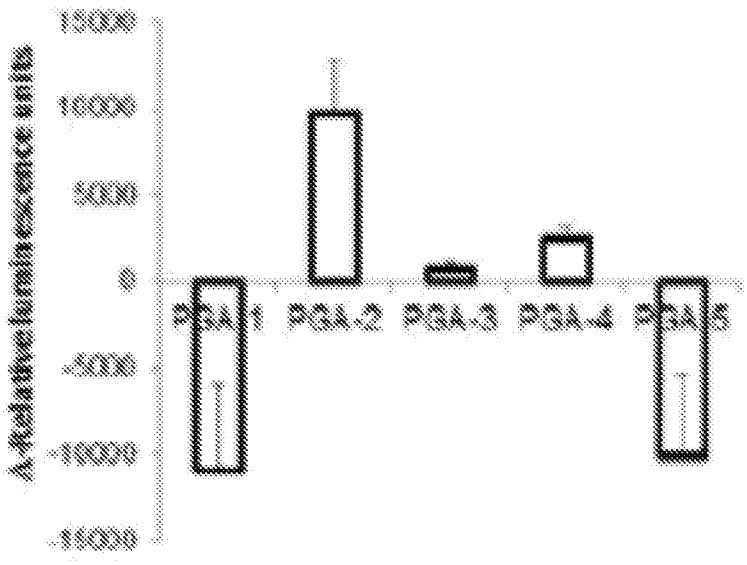

FIG. 11A

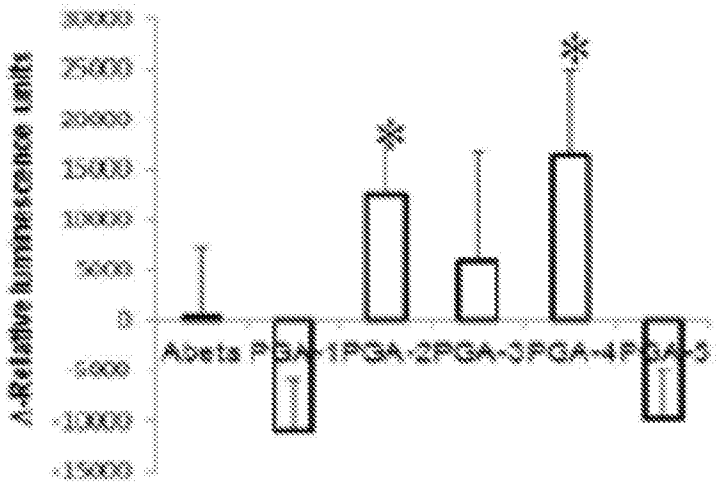

FIG. 11B

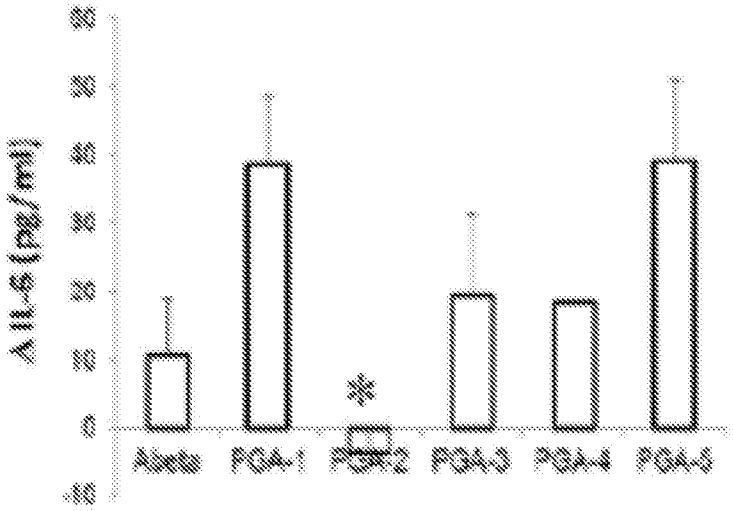

FIG. 11C

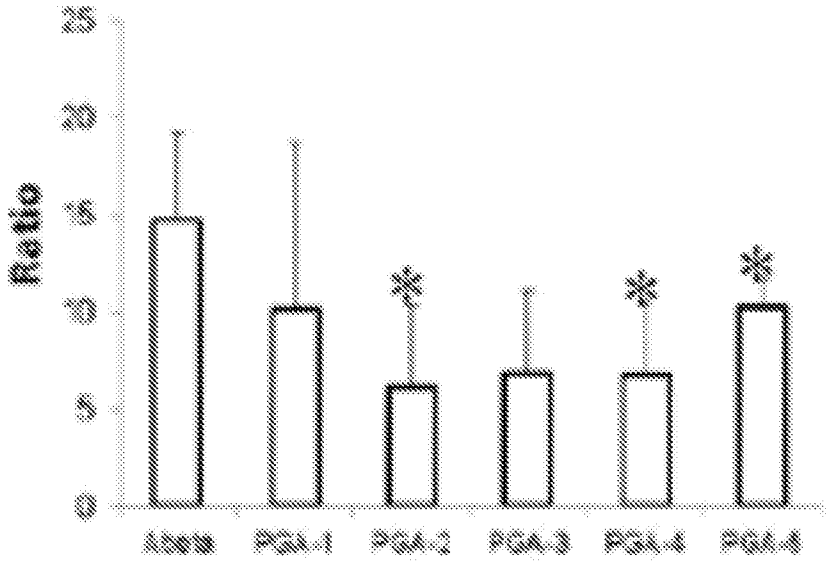

FIG. 11D

	Structural similarity RMSD		Docking features					% PP$_{II}$		# of rotatable bonds		Log P		K$_d$ μM		IC$_{50}$ μM		% apoptosis at IC$_{50}$		Estimated LD$_{50}$ (mg/kg)		Overall rank
	WT GILZ		PP$_{II}$		% TAT		%TAZ															
	≤ 3	> 3	≤ 3	> 3	≥35	<35	<35	≥ 26	< 26	≤ 10	> 10	≤ 6	> 6	≤ 3	> 3	≤ 2	> 2	≤ 26	> 26	> 1600	≤ 1600	
PGA-2	1	0	0		1		1	1	0	1	0	0	0	1	0	1	0	1	0	1	0	6
PGA-3	1		1		1		0			1	0							1	0	1	0	8
PGA-5		0		0		0	0	1	0	1	0	1	0	1	0	1	0	1	0	1	0	5
PGA-4	1		1		1		0			1	0	1	0	1	0	1	0	1	0	1	0	8
PGA-6	1		1		1		1	1	0	0	0	0	0	1	0	1	0	1	0	1	0	8

FIG. 12

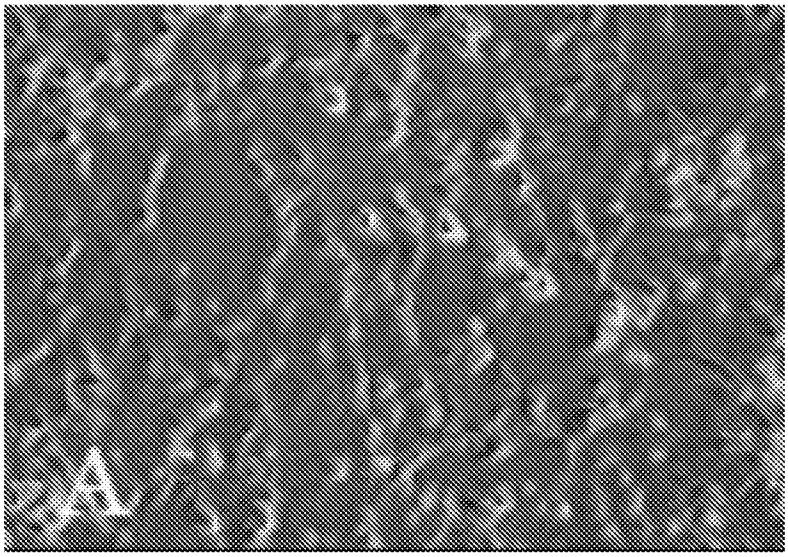

FIG. 13A

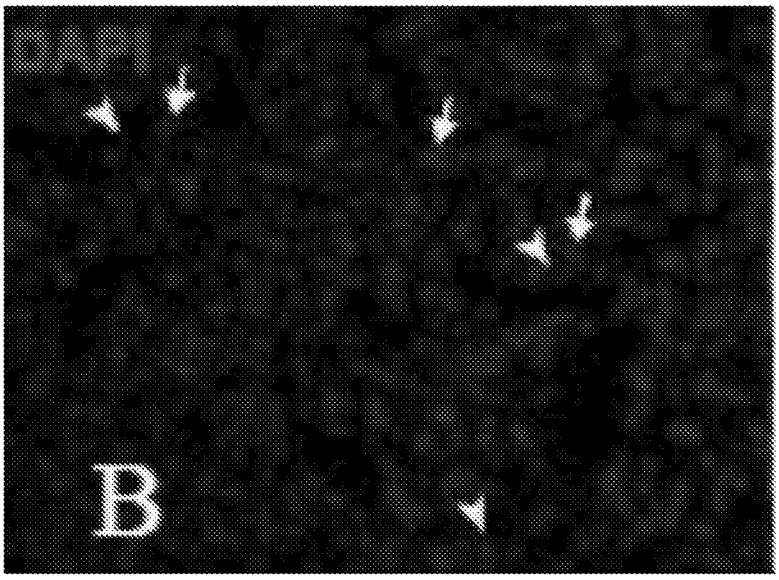

FIG. 13B

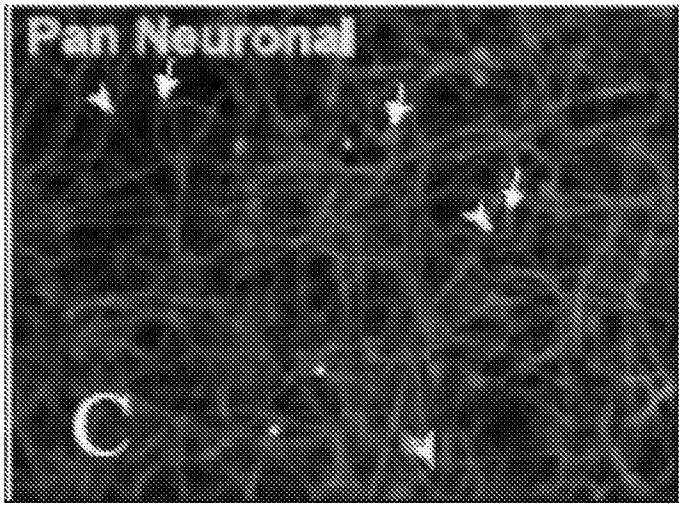

FIG. 13C

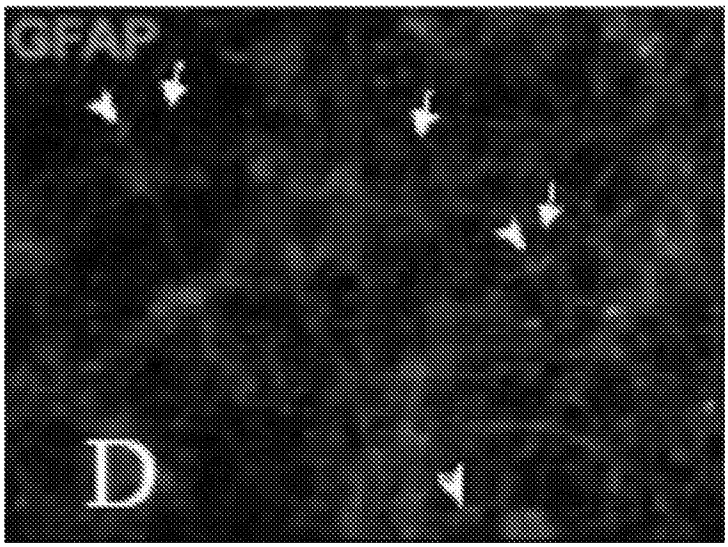

FIG. 13D

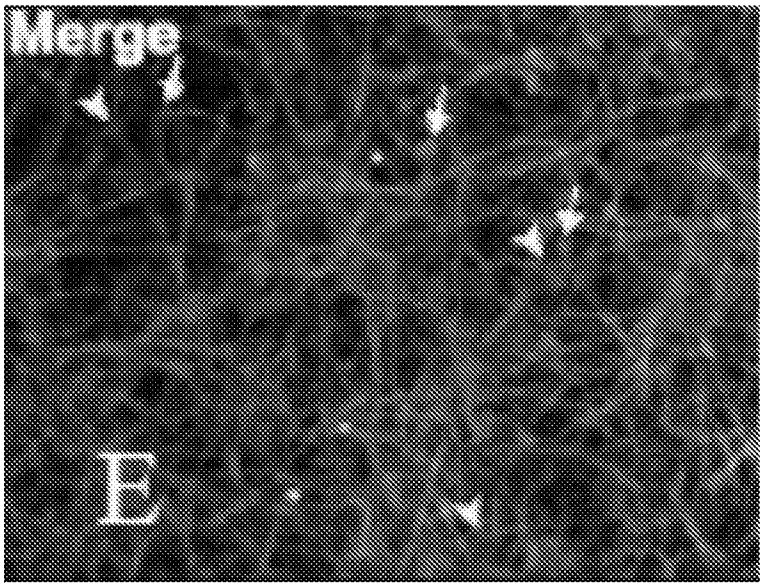

FIG. 13E

INTERNATIONAL SEARCH REPORT

International application No.
PCT/US 17/18645

A. CLASSIFICATION OF SUBJECT MATTER
IPC(8) - A61K 38/00 (2017.01)
CPC - C07K 4/00, C07K 4/12, C07K 2319/00, C07K 7/00

According to International Patent Classification (IPC) or to both national classification and IPC

B. FIELDS SEARCHED

Minimum documentation searched (classification system followed by classification symbols)
See Search History Document

Documentation searched other than minimum documentation to the extent that such documents are included in the fields searched
See Search History Document

Electronic data base consulted during the international search (name of data base and, where practicable, search terms used)
See Search History Document

C. DOCUMENTS CONSIDERED TO BE RELEVANT

Category*	Citation of document, with indication, where appropriate, of the relevant passages	Relevant to claim No.
X --- Y --- A	US 2014/0186372 A1 (ALTMAN et al.) 03 July 2014 (03.07.2014) para [0040], [0116]	1-3, 35-41 ----- 4, 33, 34 ------ 16
Y ---- A	US 2013/0330335 A1 (BREMEL et al.) 12 December 2013 (12.12.2013) para [0045], [0277], SEQ ID NOs: 7192 and 7894	4 ---- 16
Y	Zafar et al. Chromatinized Protein Kinase C-theta Directly Regulates Inducible Genes in Epithelial to Mesenchymal Transition and Breast Cancer Stem Cells. Mol. Cell. Biol. (August 2014) vol. 34 no. 16, pp 2961-2980, pg 2961, col 2, para 2, pg 2977, col 2, para 2	33, 34

☐ Further documents are listed in the continuation of Box C. ☐ See patent family annex.

* Special categories of cited documents:
"A" document defining the general state of the art which is not considered to be of particular relevance
"E" earlier application or patent but published on or after the international filing date
"L" document which may throw doubts on priority claim(s) or which is cited to establish the publication date of another citation or other special reason (as specified)
"O" document referring to an oral disclosure, use, exhibition or other means
"P" document published prior to the international filing date but later than the priority date claimed
"T" later document published after the international filing date or priority date and not in conflict with the application but cited to understand the principle or theory underlying the invention
"X" document of particular relevance; the claimed invention cannot be considered novel or cannot be considered to involve an inventive step when the document is taken alone
"Y" document of particular relevance; the claimed invention cannot be considered to involve an inventive step when the document is combined with one or more other such documents, such combination being obvious to a person skilled in the art
"&" document member of the same patent family

Date of the actual completion of the international search	Date of mailing of the international search report
13 June 2017	29 JUN 2017
Name and mailing address of the ISA/US Mail Stop PCT, Attn: ISA/US, Commissioner for Patents P.O. Box 1450, Alexandria, Virginia 22313-1450 Facsimile No. 571-273-8300	Authorized officer: Lee W. Young PCT Helpdesk: 571-272-4300 PCT OSP: 571-272-7774

INTERNATIONAL SEARCH REPORT

International application No.
PCT/US 17/18645

Box No. II Observations where certain claims were found unsearchable (Continuation of item 2 of first sheet)

This international search report has not been established in respect of certain claims under Article 17(2)(a) for the following reasons:

1. ☐ Claims Nos.:
because they relate to subject matter not required to be searched by this Authority, namely:

2. ☐ Claims Nos.:
because they relate to parts of the international application that do not comply with the prescribed requirements to such an extent that no meaningful international search can be carried out, specifically:

3. ☐ Claims Nos.:
because they are dependent claims and are not drafted in accordance with the second and third sentences of Rule 6.4(a).

Box No. III Observations where unity of invention is lacking (Continuation of item 3 of first sheet)

This International Searching Authority found multiple inventions in this international application, as follows:

---------- see extra sheet ----------

1. ☐ As all required additional search fees were timely paid by the applicant, this international search report covers all searchable claims.

2. ☐ As all searchable claims could be searched without effort justifying additional fees, this Authority did not invite payment of additional fees.

3. ☐ As only some of the required additional search fees were timely paid by the applicant, this international search report covers only those claims for which fees were paid, specifically claims Nos.:

4. ☒ No required additional search fees were timely paid by the applicant. Consequently, this international search report is restricted to the invention first mentioned in the claims; it is covered by claims Nos.:
1-4, 16, and 33-41 limited to SEQ ID NOs: 1, 11

Remark on Protest

☐ The additional search fees were accompanied by the applicant's protest and, where applicable, the payment of a protest fee.

☐ The additional search fees were accompanied by the applicant's protest but the applicable protest fee was not paid within the time limit specified in the invitation.

☐ No protest accompanied the payment of additional search fees.

INTERNATIONAL SEARCH REPORT

International application No.
PCT/US 17/18645

Continuation of Box No. III, Observations where unity of invention is lacking:

This application contains the following inventions or groups of inventions which are not so linked as to form a single general inventive concept under PCT Rule 13.1. In order for all inventions to be examined, the appropriate additional examination fees must be paid.

Group I+: Claims 1-41, directed to a pharmaceutical composition comprising a polypeptide, wherein the polypeptide comprises Formula I: X1-X2-X3-P-X4-X5-P-X6-X7 or Formula II: X1-X2-X3-P-X4-X5-P-X6-X7-X8; having a tetrapeptide motif PXXP. The polypeptide will be searched to the extent that Formula I encompasses the first named species of SEQ ID NO: 1 (SEQ ID NO: 11). It is believed that claims 1-4, 16, 33-41, encompass this first named invention, and thus these claims will be searched without fee to the extent that the peptide encompasses SEQ ID NOs: 1 and 11. Additional polypeptide sequences will be searched upon the payment of additional fees. Applicants must specify the claims that encompass any additionally elected polypeptide sequences. Applicants must further indicate, if applicable, the claims which encompass the first named invention, if different than what was indicated above for this group. Failure to clearly identify how any paid additional invention fees are to be applied to the "+" group(s) will result in only the first claimed invention to be searched. An exemplary election would be a pharmaceutical composition comprising the first specifies of SEQ ID NO: 2 (SEQ ID NO: 16) (claims 1-3, 5, 21, 33-41).

Group II: Claims 42-46, directed to the use of a pharmaceutical composition for the treatment of a neurodegenerative disease in a patient

The inventions listed as Groups I+ and II do not relate to a single general inventive concept under PCT Rule 13.1 because, under PCT Rule 13.2, they lack the same or corresponding special technical features for the following reasons:

Special Technical Features

The technical feature of each of the inventions listed as Group I+ is the specific polypeptide sequences, recited therein. Each invention of Group I+ requires a specific polypeptide sequence, not required by any of the other inventions.

Group I+ does not require the use of a pharmaceutical composition for treating a neurodegenrative disease, as required by Group II.

Group II does not require an isolated pharmaceutical composition, as required for Group I+

Common Technical Features

The inventions of Group I+ and II share the technical feature of a polypeptide from 8 to 12 amino acid residues, the polypeptide comprising a tetrapeptide having the sequence of PXXP. However, this shared technical feature does not represent a contribution over prior art, in view of US 2014/0186372 A1 to Altman et al. (hereinafter 'Altman') (para [0116] "a pharmaceutical composition includes an inhibitor of binding between PKC.theta. and CD28. ... a PKC.theta. sequence includes a ARPPCLPTP sequence, a substitution of an amino acid in a ARPPCLPTP sequence (e.g., a first or last proline residue), a sequence motif set forth in Table 1, or a substitution of an amino acid in a sequence motif set forth in Table 1."; para [0166], Table 1; para [0090] "inhibitors include PKC.theta. amino acid sequence motif MOW, such as by way of example, a ARPPCLPTP or ETRPPCVPTPGK sequence or a subsequence thereof, or a sequence variant of ARPPCLPTP or ETRPPCVPTPGK, including for example ARLPCVPAP, ARLPCVPAS, AKLPHAPAP, AKPPYVPGP or TRLPYLPTP").

Another shared technical feature of the inventions of Group I+ is a polypeptide of comprising 9 to 10 amino acid residues (Formula I and II) having a tetrapeptide sequence of PXXP. Altman teaches said polypeptide (para [0090] "inhibitors include PKC.theta. amino acid sequence motif MOW, such as by way of example, a ARPPCLPTP or ETRPPCVPTPGK sequence.....")..

As the technical features were known in the art at the time of the invention, this cannot be considered special technical features that would otherwise unify the inventions.

Groups I+ and II therefore lack unity under PCT Rule 13 because they do not share the same or corresponding special technical feature.